



HAL
open science

Heteronemin, a spongean sesterterpene, inhibits TNF α -induced NF- κ B activation through proteasome inhibition and induces apoptotic cell death

Marc Schumacher, Claudia Cerella, Serge Eifes, Sébastien Chateauvieux,
Franck Morceau, Marcel Jaspars, Mario Dicato, Marc Diederich

► **To cite this version:**

Marc Schumacher, Claudia Cerella, Serge Eifes, Sébastien Chateauvieux, Franck Morceau, et al.. Heteronemin, a spongean sesterterpene, inhibits TNF α -induced NF- κ B activation through proteasome inhibition and induces apoptotic cell death. *Biochemical Pharmacology*, 2009, 79 (4), pp.610. 10.1016/j.bcp.2009.09.027 . hal-00544820

HAL Id: hal-00544820

<https://hal.science/hal-00544820>

Submitted on 9 Dec 2010

HAL is a multi-disciplinary open access archive for the deposit and dissemination of scientific research documents, whether they are published or not. The documents may come from teaching and research institutions in France or abroad, or from public or private research centers.

L'archive ouverte pluridisciplinaire **HAL**, est destinée au dépôt et à la diffusion de documents scientifiques de niveau recherche, publiés ou non, émanant des établissements d'enseignement et de recherche français ou étrangers, des laboratoires publics ou privés.

Accepted Manuscript

Title: Heteronemin, a spongean sesterterpene, inhibits TNF α -induced NF- κ B activation through proteasome inhibition and induces apoptotic cell death

Authors: Marc Schumacher, Claudia Cerella, Serge Eifes, Sébastien Chateauvieux, Franck Morceau, Marcel Jaspars, Mario Dicato, Marc Diederich



PII: S0006-2952(09)00850-8
DOI: doi:10.1016/j.bcp.2009.09.027
Reference: BCP 10344

To appear in: *BCP*

Received date: 24-7-2009
Revised date: 29-9-2009
Accepted date: 30-9-2009

Please cite this article as: Schumacher M, Cerella C, Eifes S, Chateauvieux S, Morceau F, Jaspars M, Dicato M, Diederich M, Heteronemin, a spongean sesterterpene, inhibits TNF α -induced NF- κ B activation through proteasome inhibition and induces apoptotic cell death, *Biochemical Pharmacology* (2008), doi:10.1016/j.bcp.2009.09.027

This is a PDF file of an unedited manuscript that has been accepted for publication. As a service to our customers we are providing this early version of the manuscript. The manuscript will undergo copyediting, typesetting, and review of the resulting proof before it is published in its final form. Please note that during the production process errors may be discovered which could affect the content, and all legal disclaimers that apply to the journal pertain.

1
2
3
4
5
6
7
8
9
10
11
12
13
14
15
16
17
18
19
20
21
22
23
24
25
26
27
28
29
30
31
32
33
34
35
36
37
38
39
40
41
42
43
44
45
46
47
48
49
50
51
52
53
54
55
56
57
58
59
60
61
62
63
64
65

Heteronemin, a spongian sesterterpene, inhibits TNF α -induced NF- κ B activation through proteasome inhibition and induces apoptotic cell death

Authors: Marc Schumacher^{a*}, Claudia Cerella^{a*}, Serge Eifes^{a*}, Sébastien Chateauvieux^a, Franck Morceau^a, Marcel Jaspars^b, Mario Dicato^a, Marc Diederich^a

^aLaboratoire de Biologie Moléculaire et Cellulaire du Cancer, Fondation de Recherche Cancer et Sang, Hôpital Kirchberg, 9 Rue Edward Steichen, 2540 Luxembourg, Luxembourg

^bMarine Biodiscovery Centre, Department of Chemistry, University of Aberdeen, Meston Walk, Aberdeen AB24 3UE, Scotland, U.K.

*equally contributed

Address correspondence to : Dr. Marc Diederich, Laboratoire de Biologie

Moléculaire et Cellulaire du Cancer, Hôpital Kirchberg, 9 rue Edward Steichen, L-

2540 Luxembourg, Luxembourg. Tel : +352-2468-4040 ; Fax : +352-2468-4060 ; E-

mail address : marc.diederich@lbmcc.lu

Abstract

1
2 In this study, we investigated the biological effects of heteronemin, a marine
3 sesterterpene isolated from the sponge *Hyrtios* sp. on chronic myelogenous leukemia
4 cells. To gain further insight into the molecular mechanisms triggered by this
5 compound, we initially performed DNA microarray profiling and determined which
6 genes respond to heteronemin stimulation in TNF α -treated cells and which genes
7 display an interaction effect between heteronemin and TNF α . Within the
8 differentially regulated genes, we found that heteronemin was affecting cellular
9 processes including cell cycle, apoptosis, mitogen-activated protein kinases (MAPKs)
10 pathway and the nuclear factor κ B (NF- κ B) signaling cascade.

11 We confirmed *in silico* experiments regarding NF- κ B inhibition by reporter gene
12 analysis, electrophoretic mobility shift analysis and I κ B degradation. In order to
13 assess the underlying molecular mechanisms, we determined that heteronemin
14 inhibits both trypsin and chymotrypsin-like proteasome activity at an IC 50 of 0.4 μ M.
15 Concomitant to the inhibition of the NF- κ B pathway, we also observed a reduction in
16 cellular viability. Heteronemin induces apoptosis as shown by Annexin V/propidium
17 iodide staining, nuclear morphology analysis, procaspase 3, -8 and -9 and poly(ADP-
18 ribose) polymerase (PARP) cleavage as well as truncation of Bid. Altogether, results
19 show that this compound has potential as anti-inflammatory and anti-cancer agent.
20
21
22
23
24
25
26
27
28
29
30
31
32
33
34
35
36
37
38

Keywords:

39 NF- κ B; marine natural product; anti-cancer drug discovery
40
41
42
43
44
45
46
47
48
49
50
51
52
53
54
55
56
57
58
59
60
61
62
63
64
65

1. Introduction

1
2
3
4 The number of identified natural compounds from marine sources has progressively
5 increased especially in the field of anti-cancer research [1]. Besides, over 70 percent
6 of earth surface is covered by the sea, which is the origin of life on earth and in some
7 marine ecosystems, like coral reefs, the biodiversity is higher than in rain forests [2].
8 In recent years, a large number of natural products, with promising properties, have
9 been isolated from marine sources, as reported in recent reviews [3]. In comparison to
10 synthetic drugs, nature-derived drugs have various advantages, such as specific
11 bioactivity and bioavailability, chemical structural diversity and the lack of toxic side
12 effects. Besides, around 70 percent of all anti-cancer drugs used in clinical therapy
13 were isolated from natural sources or bear a close structural relationship to
14 compounds of natural origin [4].

15
16 Due to its implications in most incurable diseases, the nuclear transcription factor κ B
17 (NF- κ B) has become one of the many investigated targets in drug discovery. Several
18 pathways of activation have been described so far. The first elucidated and the most
19 frequently investigated is the so-called canonical pathway, which can be triggered by
20 external stimuli like $\text{TNF}\alpha$. This pathway is mediated by the formation and
21 translocation into the nucleus of the dimer p50/p65, upon phosphorylation and
22 degradation of the cytoplasmic repressor I κ B protein [5]. This in turn contributes to
23 the transcription of specific target genes [6]. The target genes play a role in several
24 human diseases mainly linked to inflammation and cancer [7]. Besides, a close
25 association between NF- κ B and cancer exists. It has been published that inflammation
26 is the main cause of cancer in 20 percent of cases [8]. In most cases, NF- κ B is
27 activated and closely associated to carcinogenesis. This is related to an ability of NF-
28 κ B to promote pro-survival pathways [9]; as supported by the fact that induction of
29 apoptosis might follow the inhibition of the NF- κ B pathway [10]. In addition, an
30 aberrant NF- κ B activity is responsible for resistance to chemo- and radiotherapy [11].
31 Thus, it is not surprising that the role of NF- κ B signaling as a possible target for
32 cancer therapy was discussed in recent reviews [12].

33
34 Due to the higher susceptibility of cancer cells to treatments/agents affecting viability,
35 the majority of anti-cancer therapies currently applied in clinics is based on cytotoxic
36 treatments, acting *via* apoptosis induction. Apoptosis is an active and highly regulated
37
38
39
40
41
42
43
44
45
46
47
48
49
50
51
52
53
54
55
56
57
58
59
60
61
62
63
64
65

1
2
3
4
5
6
7
8
9
10
11
12
13
14
15
16
17
18
19
20
21
22
23
24
25
26
27
28
29
30
31
32
33
34
35
36
37
38
39
40
41
42
43
44
45
46
47
48
49
50
51
52
53
54
55
56
57
58
59
60
61
62
63
64
65

form of cell death by means of which damaged and mutated cells, potentially dangerous to the entire organism, can be eliminated. The execution of the apoptotic program may occur via the activation of different cascades of intracellular biochemical events converging in caspase-3 activation [13]. Two sets of events are commonly implicated in activating caspase-3: the extrinsic (or physiological) apoptotic pathway, triggered by stimulation of specific plasma membrane receptors (i.e., FAS) and mediated by caspase-8 activation; and the intrinsic (or mitochondrial) apoptotic pathway, which is triggered by stress-induced intracellular damages, leading to the release of cytochrome c from mitochondria and caspase-9 activation [14]. The two pathways are interconnected to amplify the apoptotic signal. Thus, caspase-8 can activate the mitochondrial pathway via truncation/activation of Bcl-2 family member Bid [15], whereas, caspase-8 can be further activated downstream to caspase-9 and -3 [16].

In the context of cancer and cancer therapy, DNA microarrays have been used so far for cancer classification [17] and to elucidate the potential mechanisms of action of cancer therapeutics respectively [18]. However, very few studies have focused so far on microarray technology for the functional profiling of natural compounds of marine origin as anti-cancer therapeutics [19].

In this study, we investigated the biological effects of the isolated marine sesterterpene heteronemin on the resistant chronic myeloid leukemia cancer cell line K562. To gain insights into the molecular mechanisms of action of the compound, we performed DNA microarray profiling of the changes in the transcriptional program induced by heteronemin. We found that the compound was able to affect several cellular processes, including cell cycle, apoptosis, mitogen-activated protein kinases (MAPKs) pathway and the nuclear factor κ B (NF- κ B) activation cascade. The potential ability of the compound to potently inhibit NF- κ B pathway and affect cell viability, as emerged from the DNA microarray profiling, was further confirmed by *in vitro* studies, thus showing heteronemin as a potent and promising inhibitor of TNF α -induced NF- κ B activation as well as an apoptosis inducer.

2. Material and Methods

2.1. Heteronemin

A sample of *Hyrtios erecta*. (phylum Porifera, class Demospongiae, order Dictyoceratida, family Thorectidae) was collected in November, 2000 from Vanuatu (15° 31.92'S, 167° 11.61'E) at a depth of 15 m, by Coral Reef Foundation scientists under contract with the US NCI. Collected material was stored at -20 °C until used. Voucher specimens are stored at the Smithsonian Institution, USA with voucher numbers 0CDN7710/C021264. The sample (sandy-green solid, 4.018 g dry weight) was extracted and partitioned as previously described [20]. The lipophilic hexane fraction was further purified on a normal phase silica HPLC-column (Phenomenex, Macclesfield Cheshire, UK) with hexane/ethyl acetate (70/30) solvent system to yield 180 mg of a white solid. This solid was identified as the sesterterpene heteronemin through its ¹H and ¹³C NMR spectra by comparison to previously reported data in literature [21] (Fig.1).

2.2. Cell culture and treatment

Chronic myeloid leukemia K562 and Jurkat (T cell leukemia) cells were cultured in RPMI 1640 medium (Lonza, Verviers, Belgium) supplemented with 10% fetal bovine serum (Lonza), penicillin (100 units/ml) and streptomycin (100 µg/ml) (Lonza). Cells were cultured in a 5% CO₂ incubator at 37°C and harvested every 3 days. For all experiments, we allowed 10 days, as the time needed to get enough cells after defrosting.

The day before treatment, four batches of cells are prepared for the control cells and treated cells in this way were not centrifuged on the day of treatment, thus avoiding a disruption in the transcriptome of cells undergoing short treatment. One hour before treatment, the cells are placed in the density of use. At T₀, cells were treated with 4 µM of heteronemin or equivalent volume of DMSO. At T+2h, cells were treated with 20ng/mL of TNF α , or equivalent volume of water. At T₀+2h40min cells were collected for RNA extraction and viability test. A control is performed in parallel for each processing time. RNA was extracted from a batch of 5 to 10E6 cells by the use of Trizol reagent (Invitrogen, Merelbeke, Belgium). RNA cleanup was performed by using the RNeasy Mini Kit (Qiagen, Venlo, Netherlands). RNA was quantified using a Nanodrop 1000 and the quality of this RNA was assessed by using the Agilent Bioanalyzer (RNA Integrity Number>9).

2.3. Microarray hybridization and feature extraction

Microarray experiments using Agilent 4112F human whole genome microarrays (Diegem, Belgium) were done according to the manufacturer's protocol with 700ng of total RNA, isolated previously, used for the preparation of cDNA probe and the preparation of Cy5- and Cy3-labeled cRNA probes. The hybridized and washed material on each glass slide was scanned with an Axon 4100B microarray scanner (Sunnyvale, CA, USA). Axon GenPix Pro software version 6.1 was used for feature extraction.

2.4. Microarray normalization and analysis

Competitive microarray hybridizations were performed using a 2x2 factorial design, by comparing TNF α - and heteronemin-treated cells respectively to untreated control-cells, and heteronemin and TNF α co-treated cells relative to TNF α treated cells alone. Experiments were performed in three biological replicates including two technical replicates. Technical replicates were hybridized as dye-swaps. Therefore each comparison corresponds to six hybridizations in total. The gene expression data were normalized and statistically analyzed using the R software package LIMMA (version 2.14.5) [22], which is part of the BioConductor project [23]. A linear model was fitted for the previously described experimental design. Additionally, the use of dye swaps in the experimental setup allowed the estimation of a probe-specific dye effect. This approach allows to remove dye-effect in the model and so to improve precision for the detection of differentially expressed genes.

The background correction was performed using the « normexp » function [24] with an offset of 100. « normexp » is a method implemented in LIMMA which allows stabilizing the variability of log-ratios as a function of signal intensity. Subsequently global loess normalization [25] was performed on the resulting log-ratios using a span of 0.4 to eliminate intensity-dependent dye-bias. Probes without related Entrez Gene ID annotations were eliminated in a subsequent step. A moderated F-test was used to test the remaining spots for significant changes in expression. The following contrasts were tested: « TNF α vs. Control », « Heteronemin vs. Control » and the interaction effect between heteronemin and TNF α . It might be noteworthy that the interaction effect allows detecting for which genes heteronemin and TNF α show an antagonistic respectively synergistic effect on the respective RNA levels.

1
2
3
4
5
6
7
8
9
10
11
12
13
14
15
16
17
18
19
20
21
22
23
24
25
26
27
28
29
30
31
32
33
34
35
36
37
38
39
40
41
42
43
44
45
46
47
48
49
50
51
52
53
54
55
56
57
58
59
60
61
62
63
64
65

Array quality weighting, by using the gene-by-gene update algorithm [26] was used to improve the quality of statistical analysis. By using a relative weighting approach for array quality, one may increase the power of statistical analysis for differential expression of genes. Furthermore, spots flagged as « not found » by GenePix were down-weighted. The spot- and array-wise weights are then combined into modified weights for every spot, which are used as weights in the linear model for differential expression analysis.

The p-values were adjusted for multiple hypotheses testing by using the Benjamini-Hochberg false discovery rate (FDR) [27]. Only spots with a FDR<0.05 and showing at least a 1.5-fold change were considered as statistically significant. In case where more than one spot on the array was related to the same gene, only the most significant spot with the highest F-statistic was considered for further analysis.

2.5. Quantitative real-time RT-PCR

Reverse transcriptions were performed on the same batch than the microarrays. The reaction was performed on 5µg of RNA with the SuperScript™ III first strand synthesis system for RT-PCR (Invitrogen).

Real time PCR was performed on 25ng of RNA equivalent, with the Mesa Green qPCR MasterMix Plus for SYBR® Assay (Eurogentec, Seraing, Belgium) according to the manufacturer's protocol, with 40 cycles and hybridisation at 60°C. Real time PCR was performed on a panel of 9 differentially expressed genes (Bbc3; Efn1; Jun; IkBa; Ninj1; Sesn2; Stc2; Vegfa and Znf184) and 3 housekeeping genes (β -actin, Gapdh and Mrps14); Differentially expressed genes were selected, for their different average signal intensities in the microarray experiments (sequences of primers in supplemental table 1).

2.6. Microarray data accessibility

The gene expression profiles reported in this paper have been deposited in the National Center for Biotechnology Information's Gene Expression Omnibus database. The accession number is GSE16026.

2.7. Pathway impact analysis

1 The lists of differentially expressed genes for the tested contrasts (“TNF α vs.
2 Control”, “Heteronemin vs. Control” and the interaction effect between heteronemin
3 and TNF α) were analyzed for impacted KEGG pathways [28] by means of the
4 Pathway Express software [29]. This tool is based on a statistical model taking into
5 account the number of regulated genes in a pathway and furthermore if the observed
6 changes are biologically meaningful.
7

8
9
10 An impact factor and a related FDR value were computed for every pathway. The
11 impact factor takes into account the fold changes of the regulated genes, the
12 overrepresentation of the group of regulated genes in a given pathway as well as the
13 structural topology of the analyzed pathway [29].
14

15
16
17 A statistical significance threshold (FDR < 0.25) was applied to detect impacted
18 pathways. Only pathways below the significance cut-off for at least one contrast
19 («TNF α vs. Control », « Heteronemin vs. TNF α » or the interaction effect between
20 Heteronemin and TNF α) will be shown.
21
22
23
24
25
26

27 **2.8. Gene Ontology Biological process enrichment analysis**

28
29 The different gene lists of up- and down-regulated genes were analyzed for
30 enrichment of biological processes by using the BioConductor package Gostats [30].
31 Conditional overrepresentation analysis for Gene Ontology (GO) Biological
32 Processes (BP) [31] for the positive and negative gene lists over the three contrasts,
33 including «TNF α vs. Control », « Heteronemin vs. TNF α » and the interaction effect
34 between heteronemin and TNF α , was performed.
35
36
37

38
39 All genes, which were tested for differential expression and having at least one
40 annotated GO BP term, were included in the gene universe for GO BP conditional
41 overrepresentation analysis. Only GO BP terms with at least 10 and less than
42 annotated 1000 genes are shown in the resulting tables to avoid to specific or
43 unspecific GO terms.
44
45
46
47
48

49 A statistical significance threshold (P-value < 0.05) was applied to detect enriched
50 biological processes.
51
52
53

54 **2.9. Enrichment analysis for *in silico* predicted transcription factor binding site motifs**

55
56 Promoters of the differentially regulated genes were screened for enriched TFBS
57 motifs using the Clover software [32]. Promoter sequences, 1000 base pairs upstream
58
59
60
61
62
63
64
65

1 and 200 base pairs downstream of the transcriptional start site, were retrieved from
2 the «Database of Transcriptional Start Sites» (DBTSS) version 6 [33, 34] and
3 scanned for TFBS motifs using the Clover software and the TransFac 2008.4 position
4 weight matrix (PWM) library [35]. Only high quality PWMs related to human
5 transcription factors were used for in silico screening.
6
7

8
9 Clover allows to detect enriched transcription factor binding site (TFBS) motifs by
10 comparing a positive promoter sequence set representing induced or repressed genes
11 in the considered microarray experiment against a set of promoters of not regulated
12 genes (the negative promoter set). As positive promoter set, the promoter sequences
13 for the induced or repressed genes in the different gene lists were used. As negative
14 promoter sequence set, promoters for all genes with related spots a) which show a
15 fold change less than 1.1 over all contrasts tested, b) which have an average signal
16 intensity above the lowest signal intensity detected for the significantly regulated
17 spots and c) for which no other spots related to the corresponding GeneID were
18 detected as significant over all contrasts, were included.
19
20

21 A statistical significance threshold ($P\text{-value} \leq 0.01$) was applied to detect
22 overrepresented TFBS motifs.
23
24

25 26 27 28 29 30 31 32 33 **2.10. Electrophoretic mobility shift assay (EMSA)**

34 K562 cells were resuspended in growth medium (RPMI/FCS 0,1%) to a final
35 concentration of 10^6 cells/mL and treated for 2h with or without heteronemin. The
36 cells were then challenged with 20ng/mL TNF α for 6h. Nuclear extracts were
37 prepared as described and stored at -80°C . The oligonucleotide NF-kappaBc
38 (consensus NF- κ B site 50-AGTTGAGGGGACTTTCCAGGC-30; Eurogentec) and
39 its complementary sequence were used as probe. The probe was hybridized and
40 labeled with [γ - ^{32}P]ATP (MP-Biomedicals, Illkirsch, France) and EMSA were
41 performed as published before [36]. Briefly, 10 μ g of nuclear extract were incubated
42 in binding buffer with the [γ - ^{32}P] ATP labeled probe for 20min. The DNA–protein
43 complexes were analyzed by electrophoresis on a 5% native polyacrylamide gel and
44 visualized by autoradiography. In immunodepletion experiments, nuclear extracts and
45 labeled probes were incubated on ice for 30 min prior to a 30 min incubation with 2
46 μ g of anti-p50 or anti-p65 antibodies (Santa Cruz Biotechnology, Boechout,
47 Belgium).
48
49
50
51
52
53
54
55
56
57
58
59
60
61
62
63
64
65

2.11. Transient transfection and luciferase reporter gene assay

Transient transfections of K562 cells were performed as previously described [36]. Briefly, 5 μ g of luciferase reporter gene construct containing five repeats of a consensus NF-kB site (Stratagene, Huissen, Netherlands) and 5 μ g Renilla luciferase plasmid (Promega, Leiden, Netherlands) were used for each pulse. Following electroporation, the cells were resuspended in growth medium (RPMI/FCS 10%) and incubated at 37°C and 5% CO₂. 20h after transfection, the cells were harvested and resuspended in growth medium (RPMI/FCS 0,1%) to a final concentration of 10⁶cells/mL and treated for 2h with or without heteronemin. The cells were then challenged with 20ng/mL TNF α for 6h. 75 μ l Dual-Glo™ Luciferase Reagent (Promega) were added to the cells for a 10 min incubation at 22°C before luciferase activity was measured. Then, 75 μ L Dual-Glo™ Stop & Glo1 Reagent (Promega) were added for 10min at 22°C in order to assay Renilla activity. Luciferase and Renilla (Promega) activities were measured using an Orion microplate luminometer (Berthold, Pforzheim, Germany) by integrating light emission for 10s. The results are expressed as a ratio of arbitrary units of firefly luciferase activity normalized to Renilla luciferase activity.

2.12. IKK kinase activity

The K-LISA IKK β Inhibitor Screening kit from Calbiochem was used for the measurement of the kinase activity. IKK-2 Inhibitor IV ([5-(p-fluorophenyl)-2-ureido]thiophene-3-carboxamide) (Calbiochem, San Diego, CA)) was used as a positive control. The assay was performed as indicated in the manufacture's protocol. The absorbance at 450 nm (with a reference wave length at 590 nm) was read using a SpectraCount UV-spectrometre (Packard, Groningen, Netherlands).

2.13. Proteasome Inhibition Activity

The Proteasome-Glo™ Chymotrypsin-Like Cell-Based Assay (Promega) was used in addition to the Trypsin-Like and Caspase-Like Assays to evaluate the three major proteolytic activities. Epoxomicin (at 5 μ M) (Sigma, Bornem, Belgium) was used as positive control. The assays were performed as indicated in the manufacture's protocol. Briefly, K562 cells (at a concentration of 10⁶ cells/ml in 0,1% FCS medium)

1
2
3
4
5
6
7
8
9
10
11
12
13
14
15
16
17
18
19
20
21
22
23
24
25
26
27
28
29
30
31
32
33
34
35
36
37
38
39
40
41
42
43
44
45
46
47
48
49
50
51
52
53
54
55
56
57
58
59
60
61
62
63
64
65

were treated with indicated concentrations of NLE. After an incubation period of 8 hours, 25×10^3 cells per well were mixed with 25 μ l of the recombined cell based reagent. After vigorous shaking (for 2 minutes) and an additional incubation period of 10 minutes at room temperature the luminescence was measured on a luminometer (Berthold). A viability assay, using the CellTiter-Glo® Luminescent Cell Viability Assay Kit from Promega, was performed in parallel to normalize the proteasome activity to the number of viable cells.

2.14. Cell viability assessment

The percentage of cell death after incubation with the test compounds was determined using the Cell Titer Glo® Luminescent Cell Viability Assay Kit (Promega). Assays were performed according to the manufacturer's instructions. Briefly, the assay determines the number of viable cells, based on the quantification of ATP, as indicator of metabolic activity, using the luciferase catalysis of luciferin to oxyluciferin and light in the presence of Mg^{2+} , ATP and oxygen. Lyophilized enzyme/substrate mixture was reconstituted with the provided buffer. Then, an equal volume of the reaction buffer was added to the medium containing K562 cells (untreated or treated with heteronemin at the indicated times). The mixture was shaken on a rocking platform for 2min, and then incubated for 10min in the dark at RT. The luminescence signal, proportional to the amount of ATP present, was quantified by using an Orion Microplate Luminometer, and converted in number of viable cells according to the manufacturer's instructions. Data were normalized to the control and reported as percentage of viable cells.

2.15. Analysis of apoptosis

a) Analysis of nuclear fragmentation. Percentage of apoptotic cells was quantified as the fraction of apoptotic nuclei, as previously described assessed by fluorescence microscopy (Leica-DM IRB microscope, Lecuit, Luxemburg) upon staining with the DNA-specific dye Hoechst 33342 (Sigma) [37]. The fraction of cells with nuclear apoptotic morphology was counted (at least 300 cells in at least three independent fields). The images were analyzed using the Image J software (<http://rsb.info.nih.gov/ij/docs/index.html>). b) Flow cytometric analysis (annexinV-FITC/propidium iodide-staining) of phosphatidylserine exposure. At the indicated times and doses of treatment, K562 cells were assayed for phosphatidylserine

1 exposure, by using the AnnexinV-FITC Apoptosis Detection Kit I® (Becton
2 Dickinson Biosciences, Erembodegem, Belgium) according to the manufacturer's
3 instructions. Stained samples were analysed by FACS (FACSCalibur, Becton
4 Dickinson, San José, CA, USA). Data were recorded using the CellQuest software
5 (<http://www.bdbiosciences.com/features/products>) for further analysis.
6
7
8
9

10 **2.16. Modulation of apoptosis**

11 The caspase inhibitors z-VAD-FMK, caspase-9 inhibitor II, caspase-8 inhibitor I,
12 were purchased by Calbiochem. They were dissolved in DMSO and added at the
13 concentration of 50µM, 1h before heteronemin addition.
14
15
16
17
18
19

20 **2.17. Extraction of cellular proteins**

21 After incubation of Jurkat cells with heteronemin at the indicated times, nuclear and
22 cytoplasmic extracts for the analysis of the translocation of the pro-inflammatory
23 factors were prepared according to [36]. Briefly, 10⁷ cells per sample were lysed in a
24 hypertonic detergent medium containing protease inhibitor cocktail (Complete®,
25 Roche, Luxembourg). The extraction was performed on ice to avoid protein
26 degradation. Alternatively, to analyse apoptotic parameters, whole cell extracts were
27 prepared using M-PER® (Mammalian Protein Extraction Reagent) (Pierce,
28 Erembodegem, Belgium) according to the manufacturer's instructions. 10⁷ cells per
29 sample were washed with PBS and the pellet was resuspended in 400µl of M-PER®
30 containing a protease inhibitor cocktail (Complete®, Roche, Luxembourg). The
31 suspension was put on a shaker with vertical agitation for 15min at +4°C, followed by
32 a centrifugation at 15000xg for 15min at +4°C for clarification. Afterwards,
33 supernatants were removed and aliquots were stored at -80°C until use.
34
35
36
37
38
39
40
41
42
43
44
45
46

47 **2.18. Western Blot analysis**

48 Proteins of total extracts were separated by size using sodium dodecyl sulfate
49 polyacrylamide gel electrophoresis (SDS-PAGE) (10%), transferred onto
50 nitrocellulose membranes and blocked with 5% non-fat milk in phosphate buffered
51 saline (PBS)-Tween overnight. Equal loading of samples was controlled using β-
52 actin, or lamin B and α-tubulin for cytosolic and nuclear extracts. Blots were then
53 incubated with the following primary antibodies: anti-β-Actin (1:5000, Sigma), anti-
54
55
56
57
58
59
60
61
62
63
64
65

1 caspase-8, anti-caspase-9 and anti-phospho-IkBa (1:1000; Cell Signaling, Leiden,
2 Netherlands), anti-PARP, anti-caspase-3, anti-Bid, anti-IkBa, anti-p65, and anti-p50
3 (1:1000; Santa Cruz Biotechnology, Boechout, Belgium). All antibodies were diluted
4 in a PBS-Tween solution containing 5% of bovine serum albumin (BSA) or 5% of
5 milk according to the providers' protocols. After incubation with the primary
6 antibodies, membranes were washed with PBS and incubated for 1h at RT with the
7 corresponding secondary antibodies following manufacturer's instructions (HRP
8 conjugated goat anti-rabbit or goat anti-mouse from Santa Cruz Biotechnology). After
9 washing with PBS-Tween, specific immunoreactive proteins were visualised by
10 autoradiography using the ECL Plus Western Blotting Detection System Kit® (GE
11 Healthcare, Roosendaal, The Netherlands).
12
13
14
15
16
17
18
19
20
21
22
23
24
25
26
27
28
29
30
31
32
33
34
35
36
37
38
39
40
41
42
43
44
45
46
47
48
49
50
51
52
53
54
55
56
57
58
59
60
61
62
63
64
65

3. Results

3.1. Heteronemin significantly impacted cell signaling pathways

In order to better understand the biological effects of heteronemin on chronic myeloid K562 cells, microarray experiments were performed as described in the Materials and Methods section. Pathway Express software was used to identify significantly modulated pathways by giving a particular focus on inflammation, cell death and cell cycle related pathways. Here it is noteworthy that the MAPK pathway is of particular interest, as it is known to be involved in the regulation of a large panel of cellular processes, including the regulation of inflammation and cell death. As can be seen in Table 1 the « MAPK signaling pathway » pathway was significantly impacted considering the list of differentially expressed gene for the « Heteronemin vs. Control » comparison and for the interaction effect between heteronemin and TNF α . Furthermore, the “Cell cycle” and the « Apoptosis » pathway were significantly impacted for the interaction effect between heteronemin and TNF α . Additionally, « Regulation of autophagy » was significantly modulated considering the list of differentially regulated genes comparing heteronemin-treated cells relative to untreated cells. Even though KEGG pathways are manually curated pathways, they might not encompass all related genes for a considered biological process, like for example cell death or cell cycle. The GO BP ontology allows taking a broader focus on cellular processes even though the GO BP terms take not into account the precise relationships and dependencies between the related genes.

3.2 Technical validation of microarray-data by real-time RT-PCR

We assessed the quality of the microarray experiments by quantitative real-time RT-PCR. These experiments were performed on all samples extracted from the 3 replicates. Only genes that were detected as differentially expressed were taken into consideration for quality assessment purposes by RT-PCR. These genes were selected randomly, among genes presenting different average signal intensities in the microarray experiments. Results of realtime PCR were transposed in *base 2 logarithms* in order to have comparable scales of values. Analysis of the fold changes obtained by microarray and RT-PCR for the selected genes (Table 2) shows a good correlation between the microarray and the RT-PCR platforms ($R^2=0,7734$).

1 This approach allows validating the efficiency of the microarrays experiments
2 performed.

3.3. Heteronemin modulated biological functions

4
5 To confirm the previous results and to gain further insights into the biological effects
6 of heteronemin, overrepresentation analysis for Gene Ontology Biological Processes
7 was performed. A large number of processes was found to be associated to the lists of
8 up- and down-regulated genes for the different comparisons (supplemental Table 2).
9 By visual inspection we detected a large panel of themes among the enriched GO BP
10 terms in the heteronemin related gene lists, which are related to cell cycle, cell death,
11 the MAPK pathway and the activation cascade for the transcription factor NF- κ B
12 (Table 3).
13
14

15 For the « Heteronemin vs. Control » comparison, the list of significantly down-
16 regulated genes is associated with different cell death related GO BP terms, including
17 « anti-apoptosis », « regulation of apoptosis » and « programmed cell death ».
18 Furthermore, the list of repressed genes is also associated significantly to different
19 cell cycle related GO BP terms, including « cell division » and « regulation of cyclin-
20 dependent protein kinase activity ».
21

22 As for the list of repressed genes, the list of significantly induced genes for the
23 « Heteronemin vs. Control » comparison shows an enrichment of genes related to cell
24 death, including « cell death », « positive regulation of programmed cell death »,
25 « apoptosis », « induction of apoptosis », « caspase activation », « regulation of
26 apoptosis » and « regulation of caspase activity ». Additionally topics related to cell
27 cycle including « cell cycle arrest » and « cell cycle » were found to be associated to
28 the induced gene list. Furthermore a significant association of the NF- κ B activation
29 cascade related GO term « regulation of NF-kappaB import into nucleus » was found
30 in this gene list.
31

32 The results obtained here, by comparing RNA levels of heteronemin-treated relative
33 to untreated K562 cells, suggest a modulatory effect of heteronemin on apoptosis, cell
34 cycle and the NF- κ B activation cascade.
35

36 For the lists of differentially expressed genes, considering the interaction effect of
37 heteronemin and TNF α , significant associations for the cell death related topics were
38 found with the list of negatively regulated genes, including « cell death », « negative
39
40
41
42
43
44
45
46
47
48
49
50
51
52
53
54
55
56
57
58
59
60
61
62
63
64
65

1 regulation of programmed cell death », « anti-apoptosis », « induction of apoptosis »,
2 « regulation of apoptosis », « positive regulation of programmed cell death », «
3 caspase activation », « regulation of caspase activity », « apoptosis », « DNA damage
4 response, signal transduction resulting in induction of apoptosis » and « induction of
5 apoptosis via death domain receptors ». Different GO BP terms which point to an
6 antagonistic effect of heteronemin and TNF α on cell cycle were also detected,
7 including « interphase of mitotic cell cycle », « positive regulation of mitosis » and «
8 S phase ». Furthermore MAPK pathway and NF- κ B activation cascade related GO
9 terms, including « positive regulation of JNK cascade », « I-kappaB kinase/NF-kappaB
10 cascade » and « positive regulation of NF-kappaB transcription factor activity » were
11 also found among the enriched biological topics in the list of genes showing a
12 negative interaction effect between heteronemin and TNF α . It is noteworthy, that only
13 one gene, TNF α itself is associated with the « positive regulation of JNK cascade »
14 term in the considered gene list.
15
16

17 Interestingly, no cell death, cell cycle, MAPK pathway or NF- κ B activation pathway
18 related terms were significantly associated to the list of induced genes considering the
19 interaction effect between heteronemin and TNF α .
20
21

22 Considering the lists of induced and repressed genes for the interaction contrast
23 between heteronemin and TNF α and the associated GO BP terms respectively, the
24 results suggest that both molecules have antagonistic effects on biological processes
25 and genes tightly associated to the regulation of cell death, cell cycle and the NF- κ B
26 activation cascade.
27
28

29 Altogether, the results obtained previously for pathway impact analysis and GO BP
30 enrichment analysis strongly suggest a modulatory effect of heteronemin on cell death
31 and cell cycle as well as the MAPK pathway and the NF- κ B activation cascade.
32
33

34 **3.4. Heteronemin regulated inflammation related transcription factors**

35 To uncover transcriptional regulators modulated by heteronemin, overrepresentation
36 analysis for TFBS was performed. A specific aim here was to see if inflammatory
37 response related TFBS were significantly enriched.
38
39

40 The lists of differentially expressed genes were compared to a reference list based on
41 the in silico predictions of TFBS using the high quality set of PWMs related to human
42
43
44
45
46
47
48
49
50
51
52
53
54
55
56
57
58
59
60
61
62
63
64
65

1 transcription factors from TransFac 2008.4. A complete listing of statistically
2 significantly enriched TFBS motifs can be found in supplemental table 3.

3
4 As shown in Table 4 significant associations between the negative gene list for the «
5 Interaction Heteronemin:TNF α » contrast and a large panel of NF- κ B specific PWMs
6 were detected, including V\$CREL_01, V\$NFKAPPAB_01, V\$NFKAPPAB65_01,
7 V\$NFKB_C, V\$NFKB_Q6 and V\$NFKB_Q6_01. Additionally, as can be seen in
8 supplemental table 3 no enriched NF- κ B related PWMs were detected for the list of
9 up-regulated genes considering the « Interaction Heteronemin:TNF α » contrast and
10 for the lists of up- and down-regulated genes when comparing heteronemin-treated
11 K562 cells to untreated cells, while for the « TNF α vs. Control» comparison a
12 significant association of NF- κ B specific PWMs were found with the list of induced
13 genes, including V\$CREL_01, V\$NFKAPPAB_01, V\$NFKAPPAB50_01,
14 V\$NFKAPPAB65_01, V\$NFKB_C, V\$NFKB_Q6 and V\$NFKB_Q6_01.
15
16

17 These results together with the results obtained for the enrichment analysis of GO BP
18 terms, suggest an inhibition of the activation cascade for the transcription factor NF-
19 κ B following TNF α alpha-mediated activation of this factor in K562 cells which
20 results in a downstream transcriptional repression of its direct target genes.
21
22
23

24 **3.5. Heteronemin significantly inhibited TNF α -induced NF- κ B pathway** 25 **activation**

26 The use of high-throughput profiling to identify the changes in gene expression
27 induced by heteronemin in chronic myeloid leukemia K562 cells revealed a potential
28 effect on inflammation and cell death.
29

30 First, we investigated the potential ability of heteronemin to modulate inflammation
31 by analyzing its impact on a pro-inflammatory pathway model represented by TNF α -
32 induced transcriptional activity of NF- κ B. To this purpose, as first approach, we used
33 a luciferase reporter gene assay.
34

35 Transfected cells were pre-treated for 2h with different concentrations of heteronemin
36 (Fig.2A) and challenged for 6h with 20ng/mL of TNF α . The results showed that
37 heteronemin reduced TNF α -induced NF- κ B activation in a dose-dependent manner
38 (Fig.2A), starting from a concentration of 4.0 μ M.
39

40 To confirm the inhibitory effects of heteronemin on the TNF α -induced NF- κ B
41
42
43
44
45
46
47
48
49
50
51
52
53
54
55
56
57
58
59
60
61
62
63
64
65

1 pathway, we investigated any ability of heteronemin to interfere with the NF- κ B
2 DNA binding by performing an EMSA assay. Fig.2B show that heteronemin inhibited
3 TNF α -induced NF- κ B-DNA binding, thus achieving a complete inhibition starting
4 from 4.0 μ M in K562 cells. Incubation with p50 or p65 antibodies led to the
5 identification of the p50/p65 dimer. Competition experiments with unlabeled NF- κ B
6 probes resulted in a complete disappearance of the band. Similar results are achieved
7 for Jurkat cell line (Fig. 2C).

8
9
10
11
12 As activation of NF- κ B is initiated by degradation of the natural inhibitor I κ B α , we
13 next assessed integrity of I κ B α as well as the translocation of p50 and p65 to the
14 nucleus by Western blot analysis. To this purpose, we used Jurkat cells, a system
15 model previously deeply investigated in parallel to K562 in our lab for NF- κ B studies
16 [20, 38]. First of all, we confirmed that heteronemin was able to inhibit TNF α -
17 induced NF- κ B activation in a dose-dependent manner by luciferase assay (Fig.3A).
18 Next, Jurkat cells were pretreated for 2h with 5.6 μ M heteronemin, then challenged
19 with 20ng/mL TNF α and the translocation into the nucleus of p65 and p50 together
20 with the analysis of I κ B α degradation were analyzed by WB (Fig.3B). In TNF α -
21 stimulated cells, I κ B α degradation occurs starting from 15min; concomitantly, the
22 translocation to the nucleus of NF- κ B subunits p50 and p65 was observed (Fig. 3B,
23 left). Heteronemin (Fig. 3B, right) completely prevented TNF α -induced degradation
24 of I κ B α and the subsequent translocation of p50 and p65 to the nucleus. Furthermore,
25 use of phospho-I κ B α antibody indicated that TNF α stimulated the phosphorylation of
26 I κ B α with a maximum at 10 minutes (Fig 3C, left). Heteronemin (Fig. 3C, right)
27 strongly attenuates the I κ B α phosphorylation.

28
29
30
31
32 As degradation of I κ B α depend either on IKK or proteasome activity, we then
33 determined the inhibition potential of heteronemin on IKK β activity and the
34 proteasome activity using two assays (Fig.4). First, the level of IKK β activity in
35 presence of heteronemin was monitored using an I κ B α substrate and IKK β
36 His-Tag $\text{\textcircled{R}}$. We showed that heteronemin did not significantly inhibit IKK β activity at
37 a concentration of 11.2 μ M (Fig.4A), a much higher concentration in contrast to the
38 examined range. Next, we evaluated the protease inhibition activity of heteronemin on
39 three different proteolytic sites (chymotrypsin- ; trypsin- and caspase- like) of the 26S
40 proteasome until the representative concentration value of 2.8 μ M. Above this value,
41
42
43
44
45
46
47
48
49
50
51
52
53
54
55
56
57
58
59
60
61
62
63
64
65

1 a plateau-effect was observed which led us to the determination of the proteasome
2 inhibition activity with doses lower than 2.8 μM (Fig.4B). The results indicated that
3 0.5 μM of heteronemin inhibited 55 % of chymotrypsin- and trypsin- like proteolytic
4 activity ($\text{IC}_{50}=0.4 \mu\text{M}$ for both) and 30 % of caspase-like activity ($\text{IC}_{50}>2.8 \mu\text{M}$).
5 Hence, heteronemin inhibited significantly proteasome activity. Altogether, these
6 results indicate an ability of heteronemin to inhibit the activation of NF- κB pathway.
7
8
9

10 **3.6. Heteronemin induced caspase-dependent apoptosis in K562 cells**

11 Next, we evaluated any impact of heteronemin on cell viability. K562 cells were
12 treated with different concentrations of heteronemin for 8h. Then, cell viability was
13 assessed by quantifying the percentage of metabolically active cells (see Materials
14 and Methods). As reported in Fig.5A, heteronemin induced cell death in a dose-
15 dependent manner in a range between 24 ± 5 and $80\pm 1\%$.
16
17

18 In order to understand whether the reduction in cell viability was due to apoptosis, we
19 tested treated cells for the appearance of typical nuclear apoptotic morphology, by
20 staining the nuclei with Hoechst and fluorescence microscope analysis. Nuclei of cells
21 treated with heteronemin underwent a typical apoptotic nuclear fragmentation
22 (Fig.5B). Figure 5C shows the corresponding kinetic analysis of apoptosis induction
23 upon heteronemin challenge, as estimated by counting the percentage of cells respect
24 the total with fragmented nuclei. The values after 8h of treatment confirmed results
25 from the cell viability test, thus indicating that the effects on the ATP quantification
26 were exclusively due to an impact on cell death and not to additional effects on cell
27 metabolism. The analysis of phosphatidylserine exposure confirmed that the cell
28 death occurred via apoptosis induction (Fig.5D).
29
30

31 Next, we evaluated whether heteronemin triggered a caspase-dependent apoptotic
32 pathway. To this purpose, the concentration of 5.6 μM was chosen for further
33 investigations. PARP, the known caspase-3 target, was cleaved as early as 4 hours of
34 treatment (Fig.6A, top). In agreement with these results, caspase-3 was activated in a
35 time-dependent manner reaching the maximum of cleavage between 6 and 8h
36 (Fig.6A, top), as expected by fluorescence microscope and FACS analysis (Fig.5B-
37 D). This was preceded by the cleavage of pro-caspase-9 and -8, two crucial players of
38 the intrinsic and extrinsic apoptotic pathway, respectively, operating upstream to
39 caspase-3 [14] (Fig.6A, bottom). Since the simultaneous cleavage of caspase-8 and -9
40
41
42
43
44
45
46
47
48
49
50
51
52
53
54
55
56
57
58
59
60
61
62
63
64
65

1 might be due to a cross talk between the two apoptotic pathways via truncation of Bid
2 [15], we investigated such a possible interference. To this purpose, we monitored the
3 appearance of the truncated form of Bid by WB analysis (Fig. 6B). We found that Bid
4 was truncated quite early, starting from 4h of treatment, thus indicating the possibility
5 of caspase-9 activation via caspase-8.
6
7

8
9 So far, we ascertained the cleavage/activation of the most implicated caspases in
10 apoptosis [14]. Next, we evaluated whether this activation was really required for the
11 effect on apoptosis, by using specific caspase-inhibitors. As shown in Fig.6C, the pan-
12 inhibitor z-VAD efficiently prevented the pro-apoptogenic activity of heteronemin;
13 specific caspase-9 and -8 inhibitors counteracted apoptosis at a similar level and more
14 strongly when co-added (Fig.6C), thus indicating the relevance of both caspases in the
15 resulting apoptosis. Altogether, these results indicated that heteronemin triggers
16 caspase-dependent apoptosis in K562 cells, involving the activation of both caspase-8
17 and-9.
18
19

20
21 K562 cells were described to be resistant to apoptosis induced by TNF α [39]. Finally,
22 we wanted to assess whether heteronemin was also able to sensitize K562 cells to the
23 apoptogenic effect of TNF α . To this purpose, K562 cells were pre-treated with
24 heteronemin at a concentration of 0.7 μ M, sufficient to affect the NF- κ B pathway
25 (Fig.2B) but only mildly the cell viability (data not shown), and then challenged with
26 TNF α . Figure 7 shows the analysis of apoptosis estimated by FACS in terms of
27 phosphatidylserine exposure. The results showed a percentage of apoptotic cells
28 treated with both TNF α and heteronemin that was higher compared to cell death
29 achieved by single treatments, thus indicating a synergistic rather than an additive
30 effect of the co-treatment. This indicates that low concentrations of heteronemin
31 sensitize K562 cells to TNF α -induced apoptosis and implies that the modulation of
32 NF- κ B pathway might be implicated.
33
34
35
36
37
38
39
40
41
42
43
44
45
46
47
48
49
50
51
52
53
54
55
56
57
58
59
60
61
62
63
64
65

4. Discussion

1
2 In this study, we show by using a DNA microarray functional profiling approach that
3 the spongean sesterterpene heteronemin modulates on a transcriptional level several
4 important pathways and processes related to cell proliferation and survival, including
5 cell cycle arrest, apoptosis, autophagy, the MAPK signalling pathway and the
6 inhibition of the NF- κ B activation cascade. Focusing our attention on the potential
7 modulation of inflammation and cell death, we confirmed by in vitro studies that
8 heteronemin is able to exert an anti-inflammatory action. The stimulation of chronic
9 myeloid leukemia K562 cells with the pro-inflammatory cytokine TNF α was our
10 model of investigation to mimic a pro-inflammatory condition involving NF- κ B
11 activation. Heteronemin completely prevents TNF α -induced NF- κ B activation, as
12 indicated by the complete prevention of both I κ B α degradation and phosphorylation
13 through inhibition of the 26S proteasome and the consequent p65 and p50 nuclear
14 translocation. In addition, we show that heteronemin deeply affects cell viability by
15 triggering caspase-dependent apoptosis. Related to the effects on cell death, the
16 compound was able to activate both initiator caspases -8 and-9, which are implicated
17 in the extrinsic and intrinsic apoptotic pathway, respectively [14]. The strong and
18 early truncation of Bid (detectable from 4h of treatment), known to occur downstream
19 to caspase-8 activation [15], indicates the existence of a cross-talk between the two
20 apoptotic pathways and suggests that the activation of the extrinsic caspase-8-
21 mediated apoptotic pathway might play a crucial and early role in the induction of
22 apoptosis by heteronemin.

23
24 Considerable work has been published on the anticancer and anti-inflammatory
25 effects of marine natural products. Several of these studies have been focused on the
26 anti-inflammatory and antitumor effects of spongean sesterterpenes in human cell
27 models. Thus, modulatory effects on apoptosis, cell cycle and the NF- κ B activation
28 cascade have already been described for different sesterterpenes, including
29 Cyclolinteinone, Ircinin-1 and Strobilin-felixinin. Cyclolinteinone, which is extracted
30 from sponge *Cacospongia linteiformis* is able to block lipopolysaccharide-induced
31 NF- κ B activation in a macrophage cell line [40]. The sesterterpene Ircinin-1 has been
32 shown to induce G1 cell cycle arrest and apoptosis in a human melanoma cell line
33 [41], while Strobilin-felixinin exerts its molecular effects by cell cycle arrest in S
34 phase and inhibition of topoisomerase I and polymerase alpha-primase [42]. The
35
36
37
38
39
40
41
42
43
44
45
46
47
48
49
50
51
52
53
54
55
56
57
58
59
60
61
62
63
64
65

1
2
3
4
5
6
7
8
9
10
11
12
13
14
15
16
17
18
19
20
21
22
23
24
25
26
27
28
29
30
31
32
33
34
35
36
37
38
39
40
41
42
43
44
45
46
47
48
49
50
51
52
53
54
55
56
57
58
59
60
61
62
63
64
65

pentacyclic core unit of heteronemin makes this molecule less flexible than the linear counter-parts. This rigid core might explain the specific bioactivity of heteronemin. In addition, the latter does not possess a lactone unit leading to Michael-addition reaction of nucleophilic cysteine sulfhydryl groups of the p65 monomer in the case of sesquiterpenes [43]. Moreover, it has to be noted that Michael acceptors are normally rejected as possible drug candidates as other proteins and glutathione might also interfere with a lactone group [43, 44].

So far, heteronemin has been characterized for its potentially anti-tubercular properties [45]. To our knowledge, this is the first time that anti-inflammatory as well as pro-apoptogenic activities have been described. In this context, this is the first study using a systems biology approach based on DNA microarrays and integrative data mining techniques for the functional profiling of a marine natural compound as a potential anticancer therapeutic.

Interestingly, heteronemin is able to massively induce apoptosis in a cell model well known to be strongly resistant to anti-cancer treatments acting via induction of apoptosis. Since the NF- κ B pathway is constitutively activated in K562 cells *via* Bcr-Abl and may be further stimulated in response to apoptogenic agents as part of a pro-survival strategy [46], at our level of investigation, we cannot exclude that the effects exerted by heteronemin on NF- κ B, may directly play a role in promoting/favouring the triggering of apoptosis. Interestingly, K562 cells that are resistant to the apoptogenic effect of TNF α [39], become sensitized when co-treated with low concentrations of heteronemin able to inhibit the NF- κ B pathway but without cytotoxicity. Results imply that the modulation of the NF- κ B pathway might be implicated in cellular resistance.

Alternatively, the modulation of the NF- κ B and apoptosis pathways may represent two faces of the same coin, conceivably being the processes independent but regulated by a common factor modulated by heteronemin. Interestingly, our functional profiling studies identify MAPK pathway as a target of heteronemin. The MAPK pathway is known to be an important regulator of NF- κ B transcription factor [47]; moreover, it is also implicated in the regulation and induction of apoptosis. These pieces of evidence suggest an implication for the MAPK signalling pathway as a possible mediator for both anti-inflammatory and pro-apoptogenic properties of

1 heteronemin and prompt us to investigate in the future the effective role played by
2 MAPKs in the biological effects of heteronemin.

3
4 The regulation of protein degradation is deeply implicated in cancer development,
5 thus the proteasome became a major target in cancer therapy. Bortezomib
6 (VELCADE®) and salinosporamide A (NPI-0052®), two novel proteasome
7 inhibitors validated this therapeutic approach. The natural γ -lactam- β -lactone NPI-
8 0052 is in clinical trials, whereas VELCADE has been approved by FDA for the
9 treatment of multiple myeloma. The response rate of the latter is 35 percent, but its
10 use is related to toxicity and drug resistance development [48-50]. Thus the discovery
11 of novel natural proteasome inhibitors could open a new point of view in this
12 promising cancer research field. As in the case of NPI-0052, heteronemin strongly
13 inhibits all three proteolytic activities; thereby a high level of proteolysis is induced.
14
15

16
17 In conclusion, in this study we delineated on a human chronic myeloid cell model
18 novel anti-inflammatory and apoptogenic properties for the spongean sesterpene
19 heteronemin, as assessed by DNA microarray profiling analysis integrated with in
20 vitro studies. This makes this compound eligible for further mechanistic studies as a
21 potential anti-inflammatory and anti-cancer agent.
22
23
24
25
26
27
28
29
30
31
32
33
34
35
36
37
38
39
40
41
42
43
44
45
46
47
48
49
50
51
52
53
54
55
56
57
58
59
60
61
62
63
64
65

Acknowledgments

1 The authors thank E Henry and J Ghelfi for technical assistance. This work was
2 supported by Télévie, the «Fondation de Recherche Cancer et Sang» and
3 «Recherches Scientifiques Luxembourg» asbl. MS, CC, SE, SC were supported by
4 Télévie grants (Fonds National de la Recherche Scientifique, Belgium). The authors
5 thank «Een Häerz fir Kriibskrank Kanner» association and the Action Lions “Vaincre
6 le Cancer” for generous support. We wish to thank the NCI Open Repository Program
7 for providing the crude extract of *Hyrtios* sp. MJ is the recipient of a BBSRC
8 Research Development Fellowship. Print costs are covered by FNR, Luxembourg.
9
10
11
12
13
14
15
16
17
18
19
20
21
22
23
24
25
26
27
28
29
30
31
32
33
34
35
36
37
38
39
40
41
42
43
44
45
46
47
48
49
50
51
52
53
54
55
56
57
58
59
60
61
62
63
64
65

Legends to figures

Figure 1: Molecular structure of Heteronemin

Figure 2: Inhibition of TNF α induced NF- κ B activation by heteronemin. K562 cells were pretreated with heteronemin at various concentrations of 2.8-7.2 μ M and incubated for 2 hours, followed by TNF α addition (at 20 ng/ml) and an additional incubation period of 6 hours. **A)** Effect of heteronemin on the inhibition of TNF α induced NF- κ B activation assessed by a Dual-GloTM Luciferase assay system on a K562 cell line. The results of the luciferase NF- κ B reporter gene assay represented the ratio of the measured luminescence of the firefly luciferase vector divided by the measured luminescence of the renilla plasmid. An untreated cell solution was the negative control, positive control was a cell solution treated with TNF α only. Results were presented as mean \pm SD of 8 individual measurements. Experiments were performed in triplicate, SD was less than 10% and typical data is shown. **B)** Effect of heteronemin on the binding affinity of NF- κ B assessed by an EMSA on K562 cells. The DNA binding affinity was determined by an incubation of the nuclear cell extract (10 μ g), prepared according to Müller and co-workers [51], with a labeled oligonucleotide probe containing the NF- κ B binding site C- κ B, with the indicated antibodies and an unlabeled NF- κ B probe (C.P.). The data shown here were representative for three independent experiments with similar results. **C)** Effect of heteronemin on the binding affinity of NF- κ B assessed by an EMSA on Jurkat cell line. One representative of three independent experiments is shown.

Figure 3: Effect of heteronemin on the degradation of I κ B α and translocation of p65 and p50 to the nucleus. **A)** Effect of heteronemin on the TNF α induced NF- κ B activation assessed by a Dual-GloTM Luciferase assay system on Jurkat cells. The results and experimental design of the luciferase NF- κ B reporter gene assay represented here is similar to Figure 1A. **B)** Jurkat cells were incubated with heteronemin (at 5.6 μ M) for 2 hours, followed by a TNF α (20 ng/ml) treatment for the indicated time periods. Cytoplasmic and nuclear extracts were prepared, fractionated on a 10% SDS-page gel, transferred to a membrane and then tested for I κ B α , p50, p65 (cytosolic) or p50 and p65 (nuclear). Equality of protein loading and

1
2
3
4
5
6
7
8
9
10
11
12
13
14
15
16
17
18
19
20
21
22
23
24
25
26
27
28
29
30
31
32
33
34
35
36
37
38
39
40
41
42
43
44
45
46
47
48
49
50
51
52
53
54
55
56
57
58
59
60
61
62
63
64
65

purity of nuclear/cytosolic extracts was checked by lamin B and α -tubulin Western Blots. The data shown here were representative for three independent experiments with similar results. **C)** Effect of heteronemin on phosphorylation of I κ B α by TNF α . A pre-treatment of heteronemin (at 5.6 μ M) for 2 hours is followed by a TNF α (20 ng/ml) treatment for the indicated time periods. Cytoplasmic extract is tested for phospho-I κ B α . Equality of protein loading and purity of nuclear/cytosolic extracts was checked by lamin B Western Blots. The data shown here were representative for three independent experiments with similar results.

Figure 4: Effect of heteronemin on the activity of IKK and proteasome activity.

A) Effect of heteronemin at the indicated concentrations on the kinase activity of IKK β for an incubation period of 30 minutes at 30°C. “no enzyme” was performed without IKK β and “negative control” was determined without any test compound but in the presence of IKK β . IKK-2 Inhibitor IV (Calbiochem) was used at the recommended concentration of 1 μ M. Results are shown as representative mean \pm SD of three individual measurements. * represents $p < 0.05$ compared to the negative control. **B)** Effect of heteronemin at the indicated concentrations on the proteolytic activity of the 26S proteasome in K562 cells. Results are shown as a ratio of the luminescence of the firefly luciferase activity of the proteasome kit (using a Proteasome-Glo™ Chymotrypsin-Like Cell-Based Assay from Promega) over the firefly luciferase activity of the viability kit (CellTiter-Glo® Luminescent Cell Viability Assay Kit from Promega) to get a standardized result associated to the number of viable cells. “Negative Control” refers to a control with no test compound. 5 μ M of the known proteasome inhibitor epoxomicin was used as positive control. Results are shown as representative mean \pm SD of three individual experiments. * and ** represent $p < 0.05$ or $p < 0.01$, respectively, compared to the negative control.

Figure 5: Heteronemin affects cell viability via apoptosis induction. A) Luciferase assay to assess the effect of heteronemin on cell viability of K562 cells. Cells were treated 8h with 5.6 μ M heteronemin. Then, the number of viable cells was determined as the number of metabolically active cells (ATP quantification). Data are depicted as mean \pm SD (n = 3). **B)** Representative image of K562 cells stained with Hoechst to detect nuclear morphology [37], untreated (right panel) vs. treated with 5.6 μ M

1 heteronemin for 8h (left panel), the latter presenting typical fragmented apoptotic
2 nuclei (white arrows). **C)** Kinetic analysis of apoptosis induced by heteronemin,
3 evaluated as the fraction of cells with apoptotic nuclei stained with Hoechst. The data
4 are the mean of $n = 3$ independent experiments \pm SD. **C)** Detection of apoptotic cells
5 after annexinV-FITC/propidium iodide (PI)-staining by FACS. The lower right
6 quadrant of the plot indicates early apoptotic cells that are only positive for annexinV.
7 One of 3 independent experiments with similar results is shown.
8
9
10
11

12
13 **Figure 6: Heteronemin triggers a caspase-dependent apoptosis.** **A)** Analysis of the
14 cleavage of pro-caspases-3, -8, -9 and PARP by Western blot. Cells were incubated
15 with the test compound and the cleavage of the protein after 2, 4, 6 and 8h was
16 investigated in comparison with a non-treated sample (CTRL). Actin was used as a
17 control of constant protein loading of samples. **B)** Assessment of the activation of Bid
18 by heteronemin in K562 cells by Western Blot analysis. One of three independent
19 experiments is shown in **A)** and **B)**. **C)** Analysis of the impact of caspases inhibitors
20 on the ability of heteronemin to trigger apoptosis. K562 cells were pre-treated 1 h
21 before with the pan-inhibitor ZVAD, caspase-9, -8, -9 +8 inhibitors, used at the
22 concentration of 50 μ M. The data are the mean of three independent experiments \pm
23 SD.
24
25
26
27
28
29
30
31
32
33
34
35
36

37 **Figure 7: Heteronemin sensitizes K562 cells to TNF α -induced apoptosis.** Effect of
38 heteronemin on TNF α -induced apoptosis. K562 cells were pre-treated two hours with
39 0.7 mM of heteronemin and then incubated for 8 hours with TNF α (20 ng/ml). The
40 data, as assessed by annexin V-FITC/PI staining and FACS analysis, are the mean of
41 three independent experiments \pm SD.
42
43
44
45
46
47
48
49
50
51
52
53
54
55
56
57
58
59
60
61
62
63
64
65

References

- 1
2
3 [1] Newman DJ, Cragg GM. Natural products as sources of new drugs over the
4 last 25 years. *J Nat Prod* 2007;70:461-77.
5 [2] Donia M, Hamann MT. Marine natural products and their potential
6 applications as anti-infective agents. *Lancet Infect Dis* 2003;3:338-48.
7 [3] Blunt JW, Copp BR, Hu WP, Munro MH, Northcote PT, Prinsep MR. Marine
8 natural products. *Nat Prod Rep* 2008;25:35-94.
9 [4] Molinski TF, Dalisay DS, Lievens SL, Saludes JP. Drug development from
10 marine natural products. *Nat Rev Drug Discov* 2009;8:69-85.
11 [5] Gilmore TD. Introduction to NF-kappaB: players, pathways, perspectives.
12 *Oncogene* 2006;25:6680-4.
13 [6] Senftleben U, Karin M. The IKK/NF-kappaB pathway. *Crit Care Med*
14 2002;30:S18-S26.
15 [7] Karin M, Greten FR. NF-kappaB: linking inflammation and immunity to
16 cancer development and progression. *Nat Rev Immunol* 2005;5:749-59.
17 [8] Coussens LM, Werb Z. Inflammation and cancer. *Nature* 2002;420:860-7.
18 [9] Perona R, Sanchez-Perez I. Signalling pathways involved in clinical
19 responses to chemotherapy. *Clin Transl Oncol* 2007;9:625-33.
20 [10] Reuter S, Eifes S, Dicato M, Aggarwal BB, Diederich M. Modulation of anti-
21 apoptotic and survival pathways by curcumin as a strategy to induce
22 apoptosis in cancer cells. *Biochem Pharmacol* 2008;76:1340-51.
23 [11] Ahn KS, Sethi G, Aggarwal BB. Reversal of chemoresistance and
24 enhancement of apoptosis by statins through down-regulation of the NF-
25 kappaB pathway. *Biochem Pharmacol* 2008;75:907-13.
26 [12] Baud V, Karin M. Is NF-kappaB a good target for cancer therapy? Hopes
27 and pitfalls. *Nat Rev Drug Discov* 2009;8:33-40.
28 [13] Coppola S, Ghibelli L. GSH extrusion and and the mitochondrial pathway
29 of apoptotic signalling. *Biochem Soc Trans* 2000;28:56-61.
30 [14] Fulda S, Debatin KM. Extrinsic versus intrinsic apoptosis pathways in
31 anticancer chemotherapy. *Oncogene* 2006;25:4798-811.
32 [15] Henshall DC, Bonislawski DP, Skradski SL, Lan JQ, Meller R, Simon RP.
33 Cleavage of bid may amplify caspase-8-induced neuronal death following
34 focally evoked limbic seizures. *Neurobiol Dis* 2001;8:568-80.
35 [16] Cha YJ, Kim HS, Rhim H, Kim BE, Jeong SW, Kim IK. Activation of caspase-8
36 in 3-deazaadenosine-induced apoptosis of U-937 cells occurs
37 downstream of caspase-3 and caspase-9 without Fas receptor-ligand
38 interaction. *Exp Mol Med* 2001;33:284-92.
39 [17] Schoch C, Kohlmann A, Schnittger S, Brors B, Dugas M, Mergenthaler S, et
40 al. Acute myeloid leukemias with reciprocal rearrangements can be
41 distinguished by specific gene expression profiles. *Proc Natl Acad Sci U S*
42 *A* 2002;99:10008-13.
43 [18] Joyner DE, Bastar JD, Randall RL. Doxorubicin induces cell senescence
44 preferentially over apoptosis in the FU-SY-1 synovial sarcoma cell line. *J*
45 *Orthop Res* 2006;24:1163-9.
46 [19] Martinez N, Sanchez-Beato M, Carnero A, Moneo V, Tercero JC, Fernandez
47 I, et al. Transcriptional signature of Ecteinascidin 743 (Yondelis,
48 Trabectedin) in human sarcoma cells explanted from chemo-naive
49 patients. *Mol Cancer Ther* 2005;4:814-23.
50
51
52
53
54
55
56
57
58
59
60
61
62
63
64
65

- 1
2
3
4
5
6
7
8
9
10
11
12
13
14
15
16
17
18
19
20
21
22
23
24
25
26
27
28
29
30
31
32
33
34
35
36
37
38
39
40
41
42
43
44
45
46
47
48
49
50
51
52
53
54
55
56
57
58
59
60
61
62
63
64
65
- [20] Folmer F, Harrison WT, Tabudravu JN, Jaspars M, Aalbersberg W, Feussner K, et al. NF-kappaB-inhibiting naphthopyrones from the Fijian echinoderm *Comanthus parvicirrus*. *J Nat Prod* 2008;71:106-11.
- [21] Kashman Y, Rudi A. The ¹³C-NMR spectrum and stereochemistry of heteronemin *Tetrahedron* 1977;33:2997-8.
- [22] Smyth GK. Linear models and empirical bayes methods for assessing differential expression in microarray experiments. *Stat Appl Genet Mol Biol* 2004;3:Article3.
- [23] Gentleman RC, Carey VJ, Bates DM, Bolstad B, Dettling M, Dudoit S, et al. Bioconductor: open software development for computational biology and bioinformatics. *Genome Biol* 2004;5:R80.
- [24] Smyth G. Limma: linear models for microarray data. In: Gentleman R, Carey V, Dudoit S, Irizarry R, Huber W, editors. *Bioinformatics and Computational Biology Solutions using R and Bioconductor*. New York: Springer, 2005. p. 397-420.
- [25] Smyth GK, Speed T. Normalization of cDNA microarray data. *Methods* 2003;31:265-73.
- [26] Ritchie ME, Diyagama D, Neilson J, van Laar R, Dobrovic A, Holloway A, et al. Empirical array quality weights in the analysis of microarray data. *BMC Bioinformatics* 2006;7:261.
- [27] Benjamini Y, Hochberg. Controlling the false discovery rate: a practical and powerful approach to multiple testing. *JR Statist Soc B* 1995;57:289-300.
- [28] Kanehisa M, Goto S, Kawashima S, Okuno Y, Hattori M. The KEGG resource for deciphering the genome. *Nucleic Acids Res* 2004;32:D277-80.
- [29] Draghici S, Khatri P, Tarca AL, Amin K, Done A, Voichita C, et al. A systems biology approach for pathway level analysis. *Genome Res* 2007;17:1537-45.
- [30] Falcon S, Gentleman R. Using GOSTats to test gene lists for GO term association. *Bioinformatics* 2007;23:257-8.
- [31] Ashburner M, Ball CA, Blake JA, Botstein D, Butler H, Cherry JM, et al. Gene ontology: tool for the unification of biology. The Gene Ontology Consortium. *Nat Genet* 2000;25:25-9.
- [32] Frith MC, Fu Y, Yu L, Chen JF, Hansen U, Weng Z. Detection of functional DNA motifs via statistical over-representation. *Nucleic Acids Res* 2004;32:1372-81.
- [33] Wakaguri H, Yamashita R, Suzuki Y, Sugano S, Nakai K. DBTSS: database of transcription start sites, progress report 2008. *Nucleic Acids Res* 2008;36:D97-101.
- [34] Suzuki Y, Yamashita R, Nakai K, Sugano S. DBTSS: DataBase of human Transcriptional Start Sites and full-length cDNAs. *Nucleic Acids Res* 2002;30:328-31.
- [35] Matys V, Kel-Margoulis OV, Fricke E, Liebich I, Land S, Barre-Dirrie A, et al. TRANSFAC and its module TRANSCOMP: transcriptional gene regulation in eukaryotes. *Nucleic Acids Res* 2006;34:D108-10.
- [36] Duvoix A, Delhalle S, Blasius R, Schnekenburger M, Morceau F, Fougere M, et al. Effect of chemopreventive agents on glutathione S-transferase P1-1 gene expression mechanisms via activating protein 1 and nuclear factor kappaB inhibition. *Biochem Pharmacol* 2004;68:1101-11.

- 1
2
3
4
5
6
7
8
9
10
11
12
13
14
15
16
17
18
19
20
21
22
23
24
25
26
27
28
29
30
31
32
33
34
35
36
37
38
39
40
41
42
43
44
45
46
47
48
49
50
51
52
53
54
55
56
57
58
59
60
61
62
63
64
65
- [37] Cerella C, Scherer C, Cristofanon S, Henry E, Anwar A, Busch C, et al. Cell cycle arrest in early mitosis and induction of caspase-dependent apoptosis in U937 cells by diallyltetrasulfide (Al₂S₄). *Apoptosis* 2009.
- [38] Folmer F, Blasius R, Morceau F, Tabudravu J, Dicato M, Jaspars M, et al. Inhibition of TNF α -induced activation of nuclear factor kappaB by kava (*Piper methysticum*) derivatives. *Biochem Pharmacol* 2006;71:1206-18.
- [39] Hietakangas V, Poukkula M, Heiskanen KM, Karvinen JT, Sistonen L, Eriksson JE. Erythroid differentiation sensitizes K562 leukemia cells to TRAIL-induced apoptosis by downregulation of c-FLIP. *Mol Cell Biol* 2003;23:1278-91.
- [40] D'Acquisto F, Lanzotti V, Carnuccio R. Cyclolinteinone, a sesterterpene from sponge *Cacospongia linteiformis*, prevents inducible nitric oxide synthase and inducible cyclo-oxygenase protein expression by blocking nuclear factor-kappaB activation in J774 macrophages. *Biochem J* 2000;346 Pt 3:793-8.
- [41] Choi HJ, Choi YH, Yee SB, Im E, Jung JH, Kim ND. Ircinin-1 induces cell cycle arrest and apoptosis in SK-MEL-2 human melanoma cells. *Mol Carcinog* 2005;44:162-73.
- [42] Jiang Y, Ahn EY, Ryu SH, Kim DK, Park JS, Kang SW, et al. Mechanism of cell cycle arrest by (8E,13Z,20Z)-strobilinin/(7E,13Z,20Z)-felixinin from a marine sponge *Psammocinia* sp. *Oncol Rep* 2005;14:957-62.
- [43] Rungeler P, Castro V, Mora G, Goren N, Vichnewski W, Pahl HL, et al. Inhibition of transcription factor NF-kappaB by sesquiterpene lactones: a proposed molecular mechanism of action. *Bioorg Med Chem* 1999;7:2343-52.
- [44] Garcia-Pineros AJ, Lindenmeyer MT, Merfort I. Role of cysteine residues of p65/NF-kappaB on the inhibition by the sesquiterpene lactone parthenolide and N-ethyl maleimide, and on its transactivating potential. *Life Sci* 2004;75:841-56.
- [45] Wonganuchitmeta SN, Yuenyongsawad S, Keawpradub N, Plubrukarn A. Antitubercular sesterterpenes from the Thai sponge *Brachiaster* sp. *J Nat Prod* 2004;67:1767-70.
- [46] Morotti A, Cilloni D, Pautasso M, Messa F, Arruga F, Defilippi I, et al. NF-kB inhibition as a strategy to enhance etoposide-induced apoptosis in K562 cell line. *Am J Hematol* 2006;81:938-45.
- [47] Kefaloyianni E, Gaitanaki C, Beis I. ERK1/2 and p38-MAPK signalling pathways, through MSK1, are involved in NF-kappaB transactivation during oxidative stress in skeletal myoblasts. *Cell Signal* 2006;18:2238-51.
- [48] Huang L, Chen CH. Proteasome regulators: activators and inhibitors. *Curr Med Chem* 2009;16:931-9.
- [49] Richardson PG, Barlogie B, Berenson J, Singhal S, Jagannath S, Irwin D, et al. A phase 2 study of bortezomib in relapsed, refractory myeloma. *N Engl J Med* 2003;348:2609-17.
- [50] Ruiz S, Krupnik Y, Keating M, Chandra J, Palladino M, McConkey D. The proteasome inhibitor NPI-0052 is a more effective inducer of apoptosis than bortezomib in lymphocytes from patients with chronic lymphocytic leukemia. *Mol Cancer Ther* 2006;5:1836-43.

- [51] Schroder HC, Steffen R, Wenger R, Ugarkovic D, Muller WE. Age-dependent increase of DNA topoisomerase II activity in quail oviduct; modulation of the nuclear matrix-associated enzyme activity by protein phosphorylation and poly(ADP-ribosyl)ation. *Mutat Res* 1989;219:283-94.

Accepted Manuscript

1
2
3
4
5
6
7
8
9
10
11
12
13
14
15
16
17
18
19
20
21
22
23
24
25
26
27
28
29
30
31
32
33
34
35
36
37
38
39
40
41
42
43
44
45
46
47
48
49
50
51
52
53
54
55
56
57
58
59
60
61
62
63
64
65

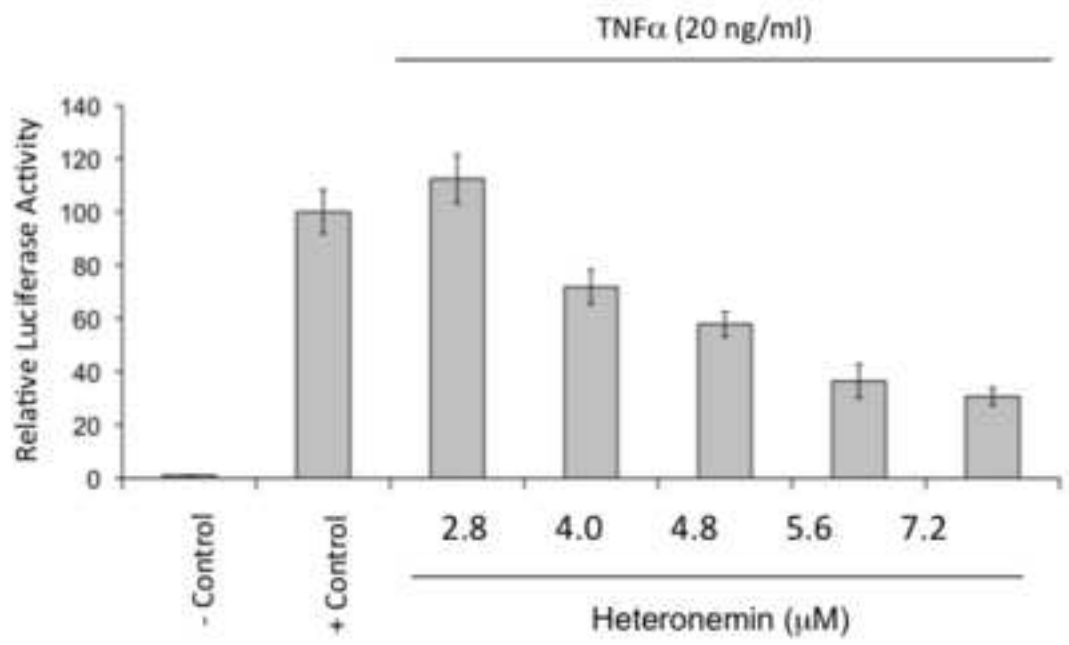
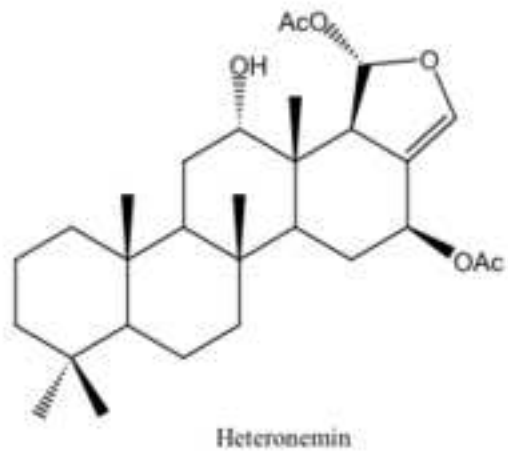


Table 1: Statistically significantly impacted KEGG pathways.

Pathways with a significant impact factor as computed by Pathway Express software are shown here. “Pathway Name” indicates the corresponding pathway name while “TNF α vs. Control”, “Heteronemin vs. Control” and « Interaction Heteronemin:TNF α » gives the corresponding impact factor. Only pathways with an FDR < 0.25 for one of the tested contrasts (« TNF α vs. Control », « Heteronemin vs. TNF α » and « Interaction Heteronemin:TNF α ») are shown. Impact factors for pathways with a FDR < 0.25 are set to boldface.

Pathway Name	TNF α vs. Control	Heteronemin vs. Control	Interaction Heteronemin:TNF α
Acute myeloid leukemia	3.537	1.433	0
Adherens junction	0	1.018	7.121
Adipocytokine signaling pathway	9.204	4.81	8.341
Allograft rejection	0	0	4.07
Apoptosis	9.461	2.967	9.627
Asthma	6.467	0	4.284
Axon guidance	4.864	0	5.405
B cell receptor signaling pathway	9.154	4.189	6.942
Base excision repair	0	0	3.467
Bladder cancer	4.169	2.726	0
Cell adhesion molecules (CAMs)	4.072	1.884	4.228
Cell cycle	3.107	4.525	2.682
Chronic myeloid leukemia	3.725	3.108	5.515
Colorectal cancer	3.029	3.385	0
Complement and coagulation cascades	5.804	1.21	0
Cytokine-cytokine receptor interaction	27.388	1.77	8.233
DNA replication	0	0	3.411
Epithelial cell signaling in Helicobacter pylori infection	16.376	10.23	7.546
Fc epsilon RI signaling pathway	4.576	0	3.356

Focal adhesion	3.652	3.746	2.215
Graft-versus-host disease	6.125	0	4.043
Hematopoietic cell lineage	9.624	1.118	3.265
Jak-STAT signaling pathway	3.146	2.799	5.095
Leukocyte transendothelial migration	6.267	0	5.218
MAPK signaling pathway	8.786	5.441	8.769
Maturity onset diabetes of the young	4.929	0	0
mTOR signaling pathway	0	5.784	0
Neurodegenerative Diseases	0	5.153	0
Natural killer cell mediated cytotoxicity	6.057	0	7.489
Nucleotide excision repair	0	0	3.237
p53 signaling pathway	5.473	11.302	4.674
Phosphatidylinositol signaling system	0	28.002	0
Prostate cancer	3.595	6.659	2.938
Regulation of autophagy	0	6.564	0
Small cell lung cancer	7.536	3.714	6.507
T cell receptor signaling pathway	16.301	3.735	8.395
TGF-beta signaling pathway	5.772	2.141	7.566
Toll-like receptor signaling pathway	19.087	4.413	5.147
Type I diabetes mellitus	3.31	0	3.942
Type II diabetes mellitus	5.389	4.473	6.814

Table 2: Correlation between Microarrays and realtime-PCR data. Results obtained with microarrays were compared to measure of the expression of a panel of 9 genes by realtime PCR. The results of realtime PCR are transposed in *base 2 logarithms* in order to have comparable scales of values. The results show a correlation of $R^2=0,7734$.

Gene Symbol	Microarray			RT-PCR		
	Het. vs Control	TNF α vs Control	Het. + TNF α vs TNF α	Het. vs Control	TNF α vs Control	Het. + TNF α vs TNF α
BBC3	2,21	0,74	1,54	2,10	0,19	2,15
EFNA1	0,04	1,27	-0,81	0,33	2,13	-1,08
JUN	2,51	1,11	1,80	3,94	0,93	2,98
NFKBIA	1,26	3,10	0,00	0,80	3,18	-0,66
NINJ1	-0,02	1,40	-0,68	-0,32	1,33	-0,86
SESN2	1,43	0,13	1,37	2,55	0,03	2,55
STC2	1,54	0,05	1,50	2,07	-0,14	2,01
VEGFA	0,67	0,02	0,84	1,72	0,08	1,95
ZNF184	0,68	-0,07	0,92	0,87	-0,28	0,77

Table 3: Statistically significantly enriched GO BP terms related to cell cycle, cell death, MAPK pathway and NF-kB activation cascade. Statistically significantly overrepresented GO BP terms (P-value < 0.05) related to selected cellular processes (cell cycle, cell death, MAPK pathway and NF-kB activation cascade) are shown for the lists of significantly up- and down-regulated genes considering the comparisons « Heteronemin vs. Control » and « Interaction Heteronemin:TNF α ». Column 1 indicates the GO BP term tested for overrepresentation. Column 2 indicates the corresponding p-value. Column 3 indicates the related gene symbols to the enriched GO BP term.

Negative gene list		
cell division	1.50E-02	CCND1, CDC26, CKS2, NDE1, SPC25
anti-apoptosis	1.66E-02	CCL2, DAD1, PRNP, SOCS3
regulation of cyclin-dependent protein kinase activity	3.09E-02	C13orf15, CKS2
regulation of apoptosis	4.07E-02	CCL2, DAD1, DYRK2, PRNP, SOCS3, SPN, UTP11L
programmed cell death	4.86E-02	CCL2, DAD1, DYRK2, PHLDA2, PRNP, SOCS3, SPN, TNFRSF12A, UTP11L
Positive gene list		
cell cycle arrest	4.24E-07	CDKN1B, DDIT3, GADD45A, HBP1, ING4, JMY, MLL5, PPP1R15A, SESN2
cell death	2.48E-05	AIFM2, BBC3, BTG1, CASP10, CDKN1B, CEBPB, CEBPG, DDIT3, DDIT4, GADD45A, IHPK2, ING4, JMY, MDM4, NFKBIA, NLRP12, PMAIP1, PPP1R15A, RFFL, SQSTM1, TNFAIP3, TRIB3, VEGFA
positive regulation of programmed cell death	5.13E-04	AIFM2, BBC3, CASP10, CDKN1B, CEBPB, CEBPG, DDIT3, IHPK2, JMY, PMAIP1
apoptosis	9.54E-04	DDIT4, GADD45A, ING4, MDM4, NFKBIA, PPP1R15A, RFFL, SQSTM1, TRIB3
induction of apoptosis	1.72E-03	AIFM2, BBC3, CASP10, CDKN1B, CEBPB, CEBPG, JMY, PMAIP1
cell cycle	5.22E-03	BOLL, CCNG2, CDKN1B, DDIT3, DUSP1, G0S2, GADD45A, HBP1, ING4, JMY, MDM4, MLL5, PPP1R15A, RGS2, SESN2, TMPRSS11A, TUBB2B

regulation of NF-kappaB import into nucleus	8.53E-03	NFKBIA, NLRP12
caspase activation	8.73E-03	BBC3, NLRP12, PMAIP1
regulation of apoptosis	1.13E-02	AIFM2, BTG1, CASP10, CDKN1B, CEBPB, CEBPG, DDIT3, IHPK2, JMY, TNFAIP3, VEGFA
regulation of caspase activity	2.00E-02	BBC3, NLRP12, PMAIP1
Interaction Heteronemin:TNFα		
Negative gene list		
cell death	1.34E-06	ABL1, BBC3, BCL3, BIRC3, CCL2, IER3, NFKBIA, PTPN6, SGPP1, TNF
negative regulation of programmed cell death	6.13E-05	BCL3, BIRC3, CCL2, IER3, TNF
anti-apoptosis	2.23E-04	BIRC3, CCL2, IER3, TNF
induction of apoptosis	5.78E-04	ABL1, BBC3, BCL3, TNF
regulation of apoptosis	1.17E-03	ABL1, BCL3, BIRC3, CCL2, IER3
positive regulation of programmed cell death	1.39E-03	ABL1, BBC3, BCL3, TNF
caspase activation	2.55E-03	BBC3, TNF
regulation of caspase activity	4.66E-03	BBC3, TNF
apoptosis	5.05E-03	NFKBIA, PTPN6, SGPP1
interphase of mitotic cell cycle	1.04E-02	ABL1, POLE
DNA damage response, signal transduction resulting in induction of apoptosis	1.94E-02	ABL1
induction of apoptosis via death domain receptors	2.11E-02	TNF
I-kappaB kinase/NF-kappaB cascade	2.44E-02	BCL3, TNF
positive regulation of JNK cascade	2.49E-02	TNF
positive regulation of mitosis	3.43E-02	TNF
S phase	3.80E-02	ABL1
positive regulation of NF-kappaB transcription factor activity	4.36E-02	TNF
Positive gene list		
/	/	/

Table 4: Statistically significantly enriched inflammatory response related TFBS. Statistically significantly overrepresented TFBS motif ($P\text{-value} \leq 0.01$), which are related to inflammatory response specific transcription factors, are shown for the lists of repressed genes considering the interaction effect between Heteronemin and $\text{TNF}\alpha$. « Matrix Name » indicates the name of the PWM used for scanning the promoter sequences for TFBS. « Transcription factor » indicates the name of the transcription factor or the family of transcription factors associated with the corresponding PWM.

Interaction Heteronemin:$\text{TNF}\alpha$		
	Matrix Name	Transcription factor
Negative gene list	V\$CREL_01	c-Rel
	V\$NFKAPPAB_01	NF-kappaB
	V\$NFKAPPAB65_01	NF-kappaB (p65)
	V\$NFKB_C	NF-kappaB
	V\$NFKB_Q6	NF-kappaB
	V\$NFKB_Q6_01	NF-kappaB

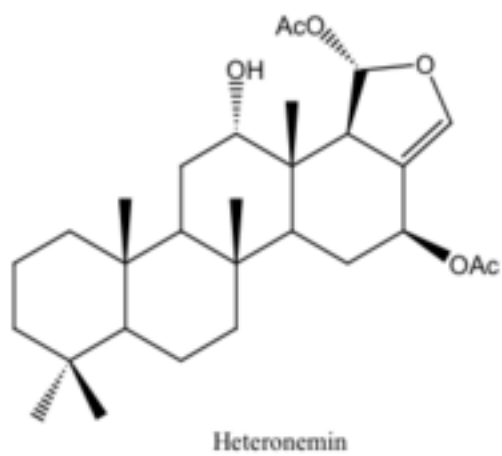


Fig.1

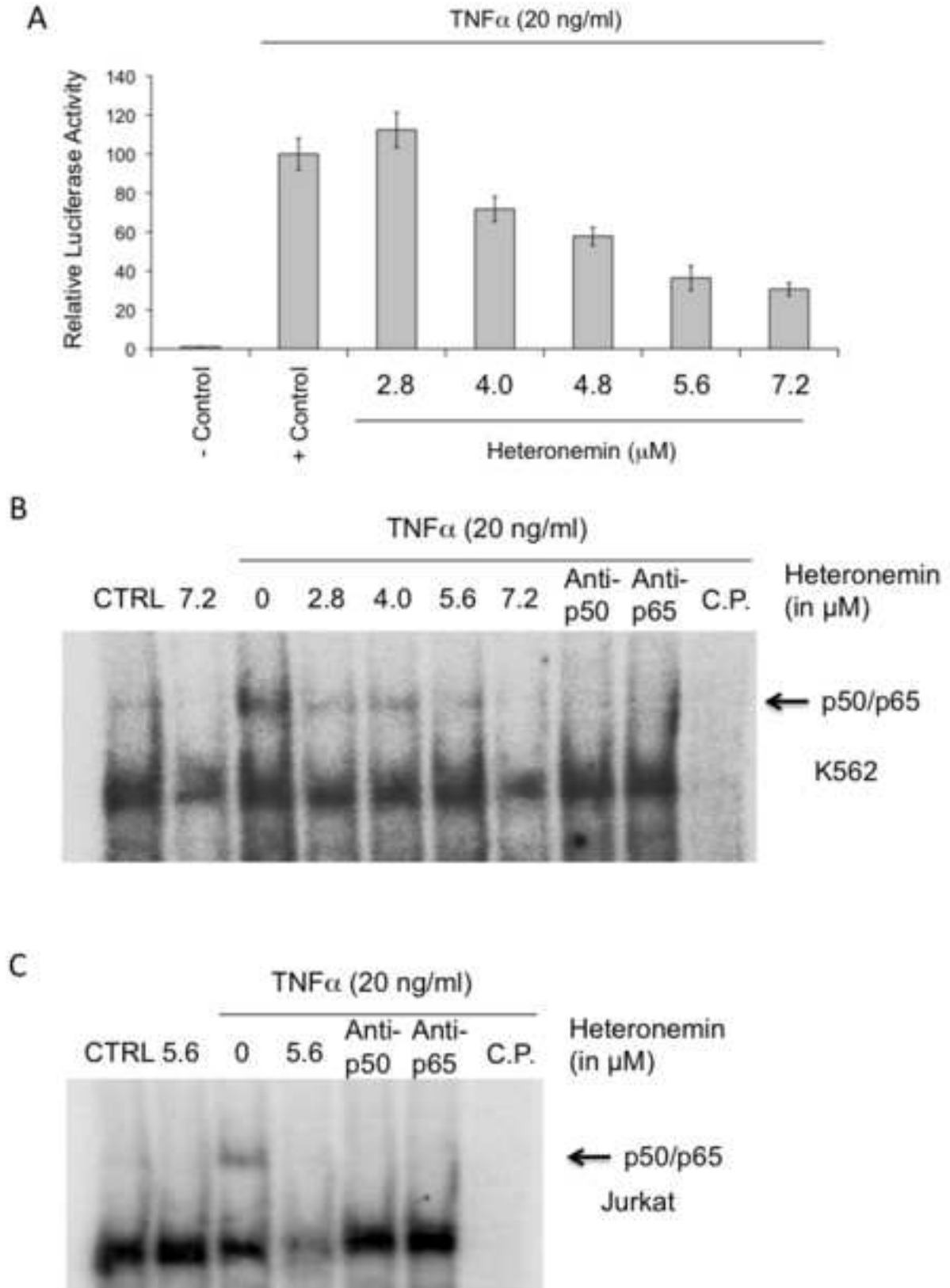


Fig.2

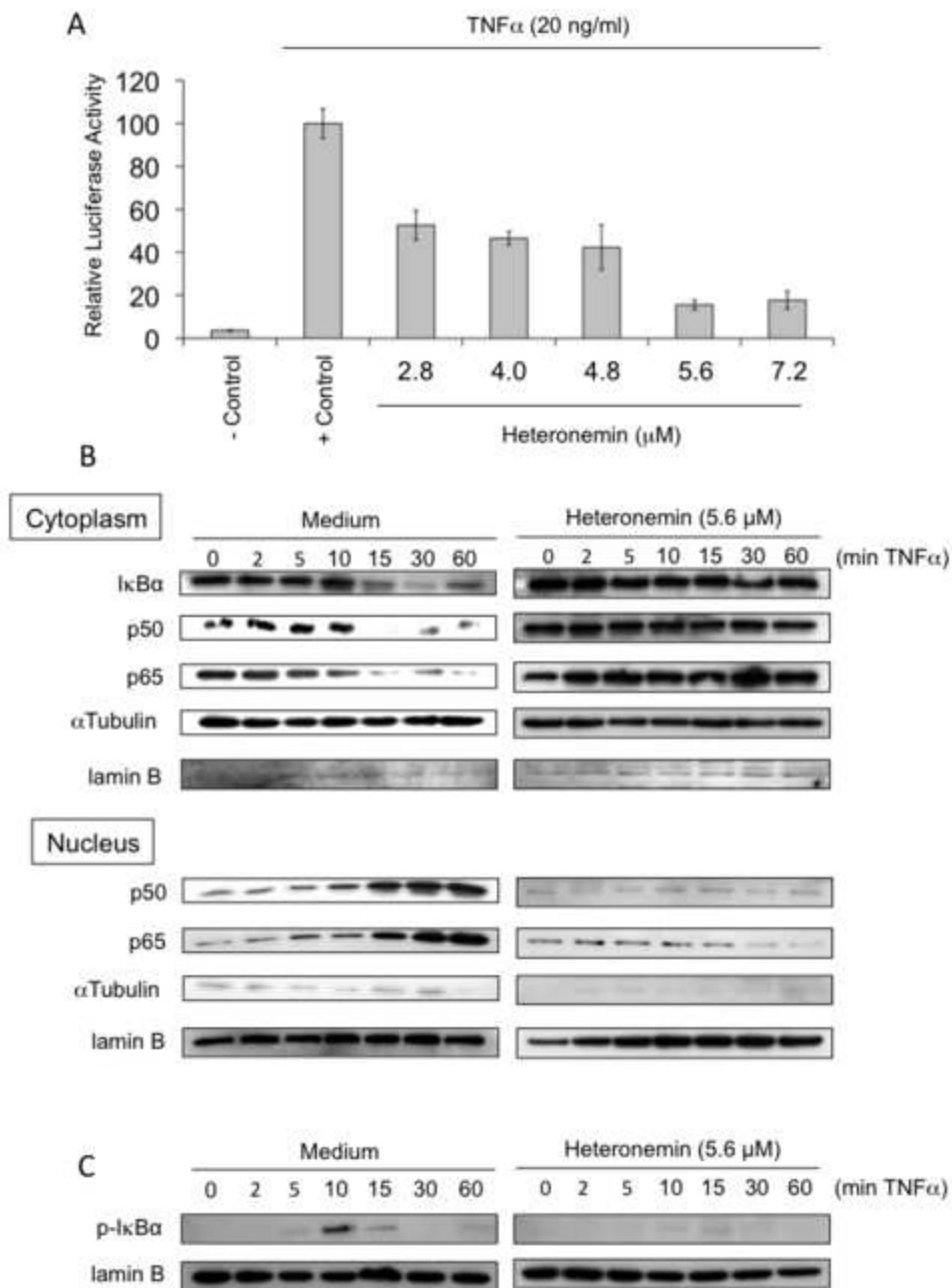
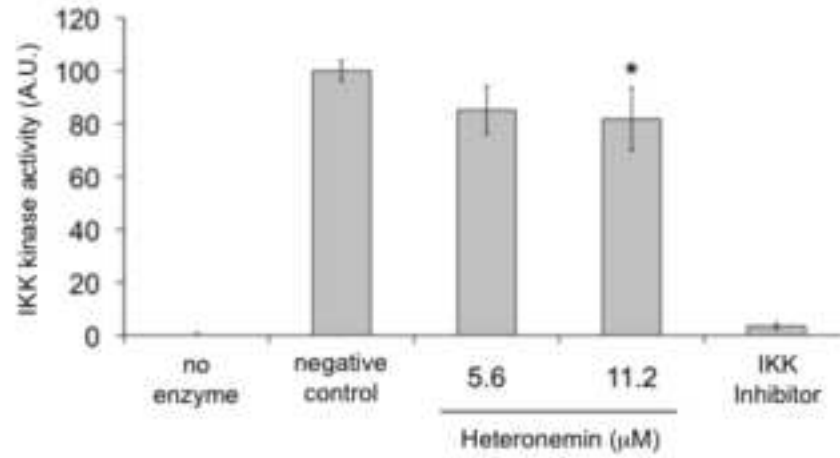


Fig.3

A



B

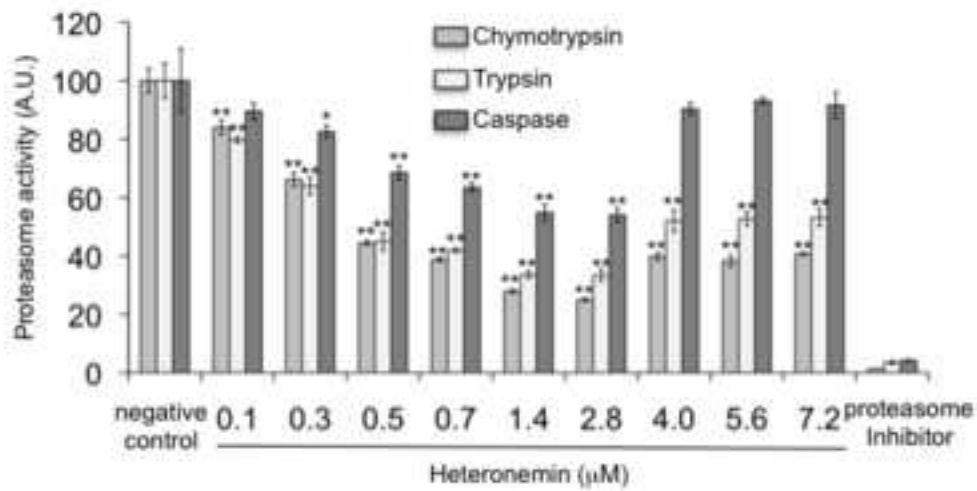


Fig.4

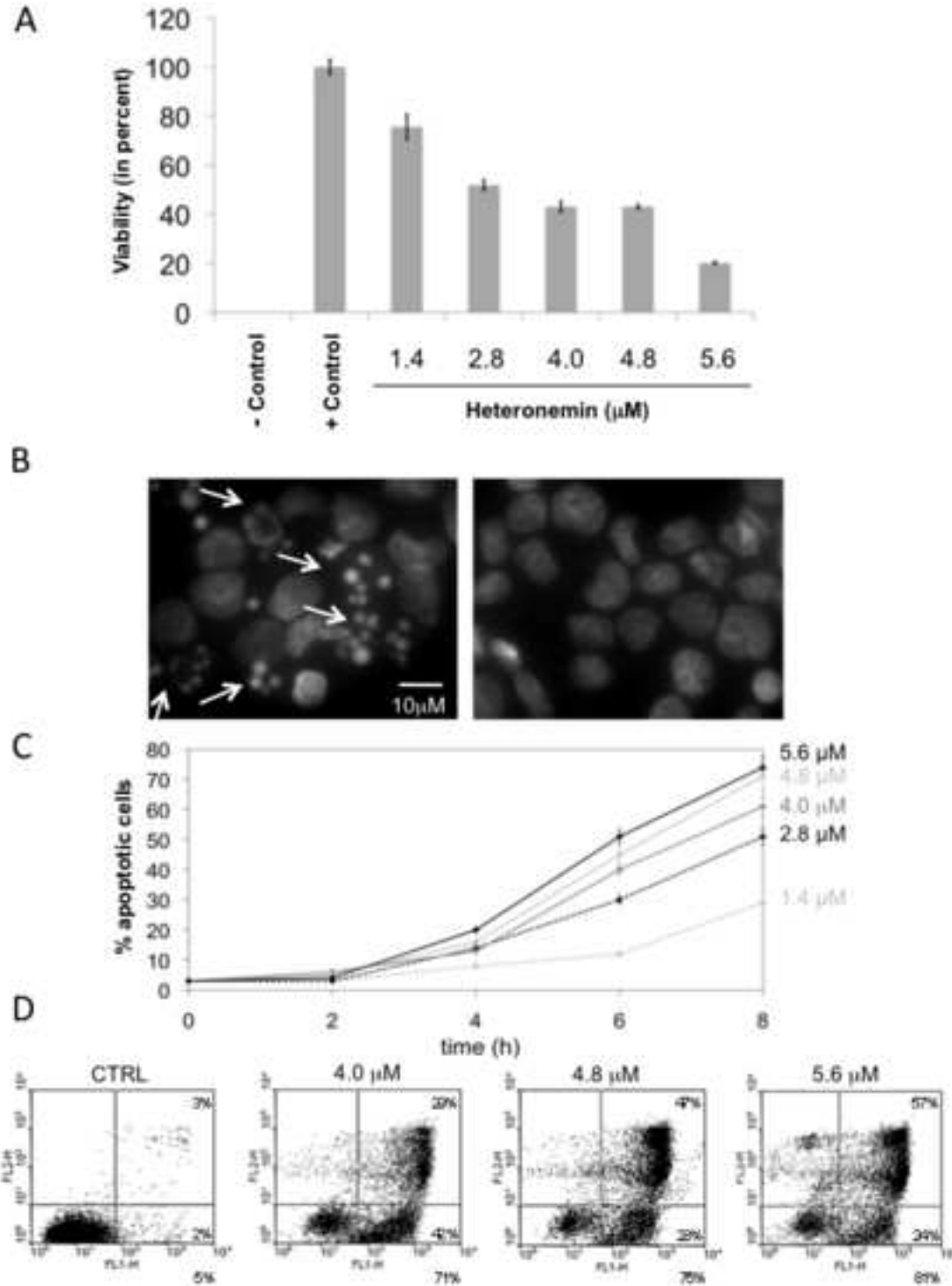


Fig.5

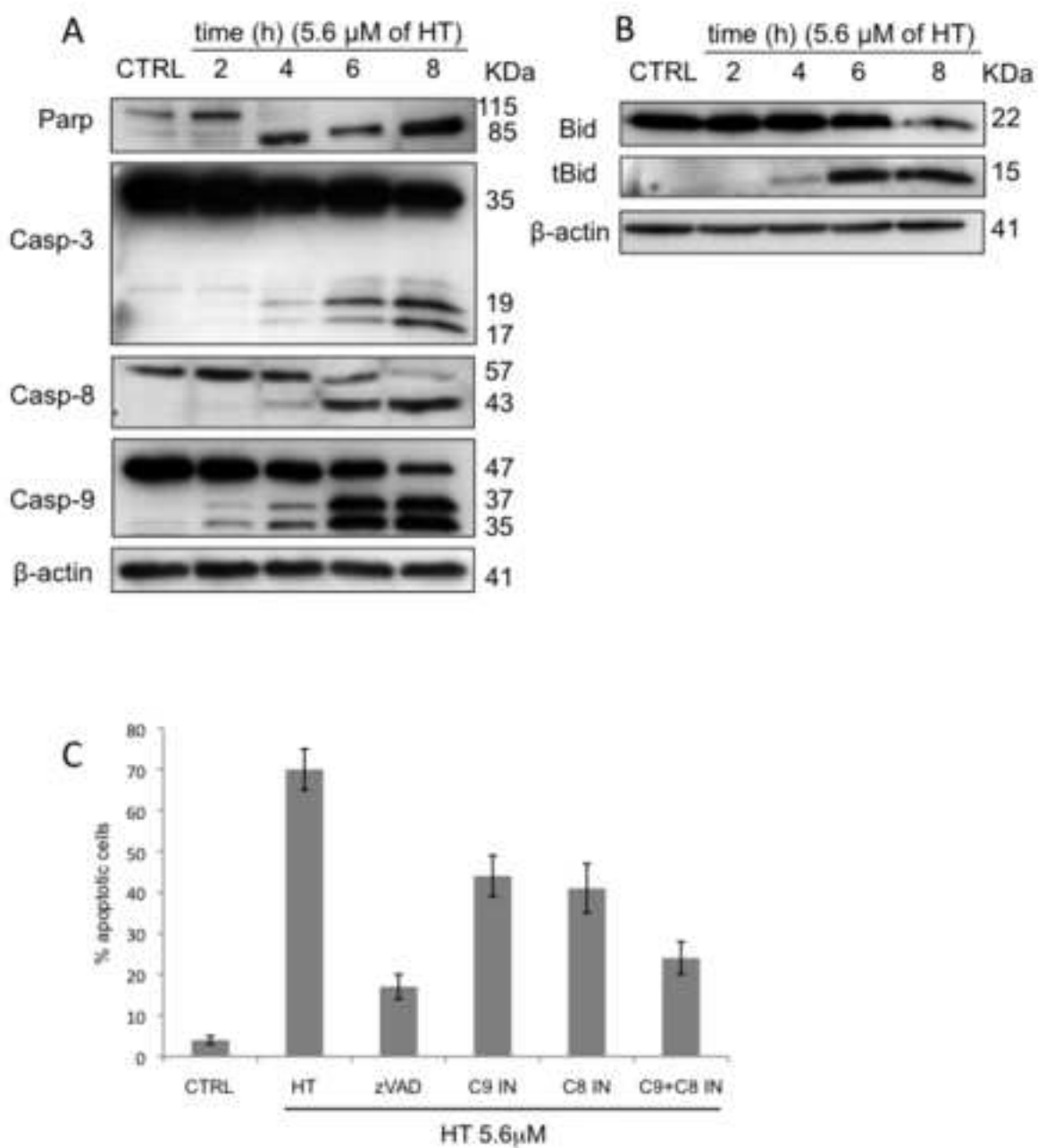


Fig.6

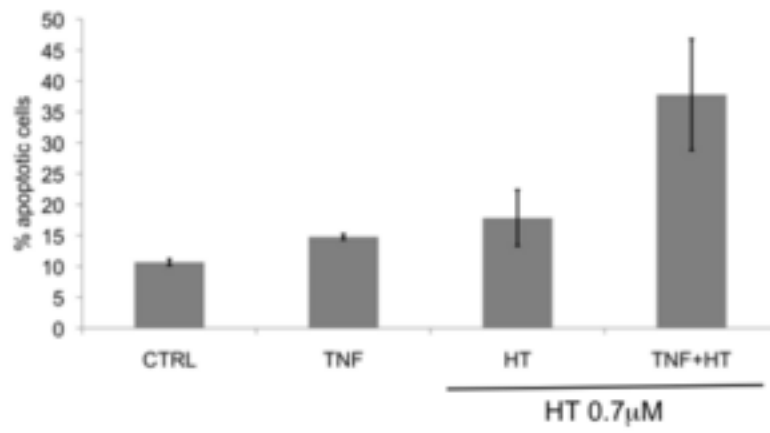


Fig.7